

NRC Research and/or Technical Assistance Report

PDR

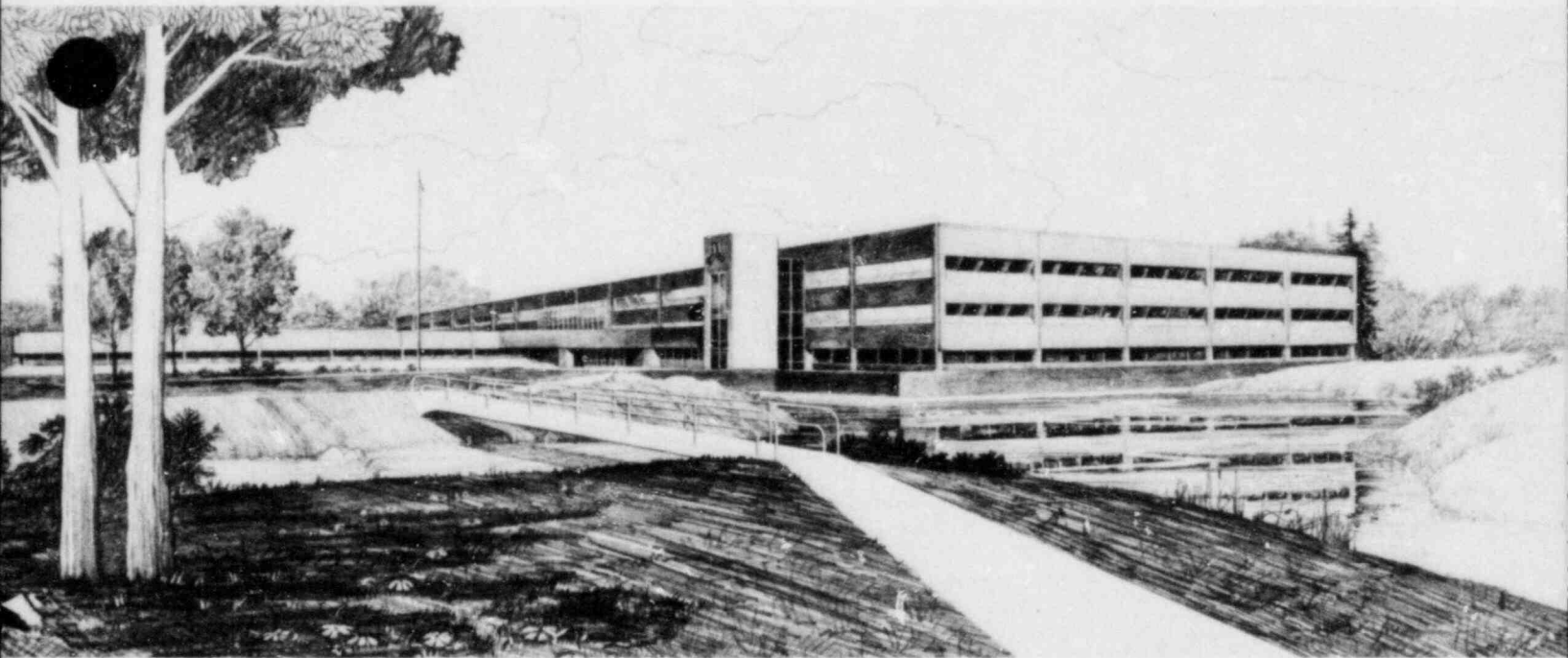
EGG-SEMI-6010
September 1982

VESSEL COOLANT MASS DEPLETION DURING A SMALL
BREAK LOCA

Mark T. Leonard

Idaho National Engineering Laboratory

Operated by the U.S. Department of Energy



This is an informal report intended for use as a preliminary or working document

Prepared for the
U.S. NUCLEAR REGULATORY COMMISSION
Under DOE Contract No. DE-AC07-76ID01570

8211100492 820930
PDR RES
8211100492 PDR



INTERIM REPORT

Accession No. _____
Report No. EGG-SEMI-6010

Contract Program or Project Title:

Semiscale

Subject of this Document:

Vessel Coolant Mass Depletion During a Small Break LOCA

Type of Document:

Topical Report

Author(s):

Mark T. Leonard

Date of Document:

September 1982

Responsible NRC Individual and NRC Office or Division:

R. R. Landry, Reactor Safety Research

This document was prepared primarily for preliminary or internal use. It has not received full review and approval. Since there may be substantive changes, this document should not be considered final.

EG&G Idaho, Inc.
Idaho Falls, Idaho 83415

Prepared for the
U.S. Nuclear Regulatory Commission
Washington, D.C.
Under DOE Contract No. DE-AC07-76 ID01570
NRC FIN No. A6038

INTERIM REPORT

ABSTRACT

The controlling phenomena associated with the depression of the reactor vessel coolant level during a small break loss of coolant accident are described. The sensitivity of core level depression during pump suction loop seal formation, exhibited in two experiments performed in the Semiscale Mod-2A facility, to core coolant bypass and steam generator secondary operation is discussed. Best-estimate computer code calculations for a pressurized water reactor are presented which show that the depth of core level depression may be very sensitive to the degree of core coolant bypass inherent in the vessel design.

FIN No. A6038
Semiscale Program

SUMMARY

Small break loss-of-coolant accidents (LOCAs) in pressurized water reactors have been investigated extensively in both experimental and analytical studies. A significant small break LOCA hydraulic phenomenon, commonly referred to as loop seal depression, has been observed in both integral and separate effects experiments. Hydraulic "seals" are formed in the pump suction loop U-bend piping as a result of the slow, gravity dominated depletion of primary coolant, characteristic of small cold leg break transients. The liquid seals impede the flow of vapor (generated in the core) through the coolant loop piping and therefore induce a differential pressure between the reactor vessel (hot legs) and downcomer (cold legs). The coolant level in the vessel is subsequently depressed, relative to the downcomer.

The lowest elevation to which the vessel level is depressed has typically been reported to correspond to the lowest elevation of the bottom of the pump suction piping (approximately 220 cm above the bottom of the core active length). A recent experiment, performed in the Semiscale Mod-2A system at the Idaho National Engineering laboratory, has shown that total core voiding is possible prior to the blowout of the pump suction liquid seals. Different controlling phenomena appear to have influenced the response in this experiment than in a previous, similar experiment.

An analysis of the experimental data has addressed several potential causes of a core liquid level depression of the observed magnitude. Although several differences in the system configuration used for this experiment, relative to that used for a previous base experiment were identified, it was concluded that a positive differential head across the primary of the intact loop steam generator during pump suction loop seal formation caused the increased core level depression. A positive differential head across the intact loop steam generator also existed in the experiment with the less severe core level depression, but not during the time that the pump loop seals were formed. It was determined that two factors acted to delay the normal drainage of coolant from the upside of

the steam generator U-tubes. First, the inherent vessel bypass flow (i.e., downcomer to upper head) had been decreased from 4.0% to 1.5%. This reduction in bypass flow diminished the steam flow from the vessel to the cold legs and increased the steam flow in the hot legs, thus impeding U-tube drainage. Second, the steam generator secondary inventory had been increased, resulting in a prolonged period of condensation in the U-tubes (over that in the previous experiment) and a consequential increase in the liquid inventory in the tubes.

The RELAP5 computer code was used to study the potential effect of core bypass flow percentage on small break behavior in a full-scale pressurizer water reactor. Over the range of break sizes and bypass flow rates calculated, a trend of increasing vessel coolant depletion with decreasing bypass flow was shown. A threshold of approximately 4.0% of the total loop flow was indicated as a lower bound of bypass flow required to prevent the depression of the vessel collapsed liquid level below the elevation of the bottom of the pump suction loop seal piping.

The significance of this study lies in the fact that the severity of a small break LOCA can be substantially increased due to the presence of a positive gravitational head in the steam generators during pump loop seal formation. In order to predict this behavior, analytical models must have the capability of calculating total and partial flooding of the U-tubes. Holdup or delayed U-tube drainage until the pump loop seals are formed are essential requirements for this phenomena to be calculated.

FOREWORD

The analysis presented in this report documents an unanticipated hydraulic phenomenon, observed in a scaled, pressurized water reactor (PWR) simulator. The observed phenomenon has changed and expanded the current understanding of the effects of pump suction loop seal behavior on vessel coolant depletion during a small break loss-of-coolant accident (LOCA).

Earlier analyses of small break LOCAs with the RELAP5 computer code yielded results for the core level response prior to pump suction loop seal blowout which were believed to be unphysical. Specifically, the collapsed level in the reactor vessel was calculated^a to be depressed to the bottom of the active core just prior to the blowout of the loop seals. These results were not immediately published because they were not fully understood and were contrary to existing scaled, integral facility experimental data. Based upon the experimental data available, the understanding of loop seal depression of the vessel liquid level was, that the lowest level reached in the core would correspond to the lowest elevation of the loop seal piping. For Westinghouse-type PWR systems, this elevation corresponds to approximately 220 cm above the bottom of the active core.

Recent experimental data have shown, however, that the calculated RELAP5 results were not altogether unphysical. Depending on plant-specific geometry and operating conditions, the collapsed level in the reactor vessel may be depressed below the lowest elevation of the pump suction piping. Full-scale PWR model calculations, as well as experimental analysis, are presented in this report which show the potential for complete core voiding prior to loop seal blowout.

a. For a full-scale PWR geometry, during a 4 inch cold leg break.

CONTENTS

ABSTRACT	ii
SUMMARY	iii
FOREWORD	v
1. INTRODUCTION	1
2. DESCRIPTION OF OBSERVED PHENOMENON	3
3. EXPERIMENTAL ANALYSIS	11
3.1 Initial Conditions	11
3.2 Transient Operational Differences	20
3.3 Vessel Upper Head Modifications	22
3.4 Bypass Flow Rate Effect	24
4. GENERALIZED PHENOMENOLOGICAL ANALYSIS	28
5. CONCLUSIONS	33
REFERENCES	35
APPENDIX A--SEMISCALE MOD-2A SYSTEM AND EXPERIMENTAL DESCRIPTION	36
APPENDIX B--CONDENSATION	41
APPENDIX C--U-TUBE FLOODING IN SEMISCALE EXPERIMENTS S-UT-6 AND S-UT-8	48

FIGURES

1. Vessel collapsed liquid level above the bottom of the core heated length	5
2. PCS mass distribution at 210 s after rupture (S-UT-6)	6
3. Intact loop steam generator differential pressure	8
4. Intact loop steam generator U-tube upflow side collapsed liquid level	9
5. PCS mass distribution at 210 s after rupture (S-UT-8)	10

6.	Intact loop steam generator secondary coolant conditions	14
7.	Broken loop steam generator secondary coolant conditions	15
8.	Vessel upper plenum pressures	16
9.	Primary/secondary fluid differential temperature (30 cm above tube sheet--upflow side)	18
10.	Intact loop steam generator U-tube upflow side collapsed liquid level	19
11.	Pressurizer and upper plenum pressures	21
12.	Vessel upper head collapsed liquid level	23
13.	Intact loop hot leg volumetric flow rate	25
14.	Intact loop hot leg average chordal densities	26
15.	Comparison of measured intact loop steam generator upflow-side U-tube collapsed liquid levels for Tests S-UT-6 and S-UT-8	27
16.	Measured and calculated vessel collapsed liquid level (Tests S-UT-6 and S-UT-8)	29
17.	PWR RELAP5 reactor vessel nodalization	30
18.	Minimum core collapsed liquid level during pump suction liquid seal formation	32
A-1.	Semiscale Mod-2A Facility (cold leg break configuration)	37
A-2.	Semiscale Mod-2A System reactor vessel assembly	38
B-1.	Primary/secondary fluid differential temperature (30 cm above tube sheet-upflow)	45
C-1.	Calculated intact loop U-tube vapor velocity and flooding velocities (S-UT-6)	50
C-2.	Calculated intact loop U-tube vapor velocity and flooding velocities (S-UT-8)	51

TABLE

1.	Experimental Initial Conditions	12
----	---------------------------------------	----

1. INTRODUCTION

The "loop seal" is a common term for the U-shaped section of piping between the steam generator outlet and pump inlet in a primary coolant loop of a pressurized water reactor (PWR). The hydraulic response of this region of the primary coolant system (PCS), during a small break LOCA, has been studied in both separate effects experiments,¹ and scaled integral facility experiments.² This report presents a new element for consideration in evaluating the effects of loop seal behavior on reactor vessel coolant depletion during a small break LOCA.

Small break LOCAs are transients which proceed slowly, such that the depletion of PCS coolant is primarily a gravity-dominated process. For the case of a cold leg break (i.e., between the PCS pump and reactor vessel downcomer), coolant accumulates in the system below the cold leg elevation. The loop seals (being below the cold leg elevation) remain liquid full as upper elevations of the system void. The loop seals, therefore, become a hydraulic plug which impedes the flow of vapor (generated in the core) to the cold legs.

Two significant transient phenomena result from the blockage of vapor flow through the loop seals. First, the coolant which exits the PCS through the break is primarily liquid. Therefore, the break mass flow rate remains high, and the volumetric flow rate low. This causes a significant loss of PCS coolant, with a slow rate of depressurization. Secondly, vapor generated in the core from decay heat has a limited volume to expand into. The pressure in the core and hot legs, therefore, increases relative to the downcomer and cold legs. The pressure differential between the hot and cold legs is manifested as a manometric coolant level imbalance between the core and downcomer. Until a pathway is cleared for vapor to flow throughout the system, the coolant collapsed level^a in the core is depressed.

a. Collapsed level is defined as the height of a single phase liquid volume required to manometrically balance a given two-phase static head.

The rate at which the core collapsed level is depressed depends on the rate at which the pressure differential between the hot and cold leg is built up which is a function of the size of the cold leg break and steam generator secondary operating conditions. The minimum collapsed level reached during the loop seal formation and clearing process is dependent upon the maximum hot to cold leg pressure differential that can be developed after the loop seals are formed. This maximum pressure differential is increased when a positive gravitational head exists across the steam generator primary (due to a difference in the upside and downside U-tube levels). It is the dependence of vessel coolant depletion (by loop seal level depression) on a positive gravitational head in the steam generator primary and potential causes of this phenomena which are discussed in this report.

2. DESCRIPTION OF OBSERVED PHENOMENON

Two similar experiments were performed in the Semiscale Mod-2A system.³ Each experiment^a simulated a 5.0%^b small break loss-of-coolant accident in a Westinghouse-type PWR.^c The initial conditions and test conduct were essentially the same for both experiments (differences in initial conditions are discussed in Section 3.1). In the first experiment (Test S-UT-6),⁴ the amount of primary coolant flow that bypassed the reactor vessel lower downcomer and core (entering the downcomer inlet annulus, and flowing through the upper head to the upper plenum) was approximately 4.0% of the total loop flow. The bypass flow for the second experiment (Test S-UT-8)⁵ was approximately 1.5% of the total loop flow. The reduced bypass flow rate was incorporated into the system configuration to improve the typicality of the Mod-2A system with respect to a full-scale PWR configuration without an upper head injection emergency core cooling system. This change was not anticipated to alter the thermal-hydraulic response of the system during a small break LOCA. A significant difference in the early hydraulic response was observed, however.

As reported in Reference 6, the reactor vessel hydraulic response during Test S-UT-6, immediately following break initiation, was characterized by rapid voiding of the upper plenum. Core boiling and coolant flashing, due to depressurization during subcooled blowdown, rapidly decreased the amount of coolant covering the core over the first 100 s of the transient. As fluid from the upper head drained into the upper plenum, the coolant level was observed to recover slightly. The vessel level was again observed to continuously decrease after 120 s when a

a. A brief description of the experimental system and the experiment operating procedures is given in Appendix A.

b. The break area was scaled to represent 5.0% of the cold leg flow area in a full-scale PWR.

c. Neither experiment was intended to exactly model the expected transient response of a Westinghouse PWR during a small break LOCA since emergency core cooling (ECC) system configurations and setpoints were atypical.

differential pressure between the core and downcomer developed, resulting from pump suction liquid seal formation. When the intact loop liquid seal was cleared at 210 s, the differential pressure was relieved and the vessel level recovered rapidly. A slow boiloff of vessel coolant then ensued until the loop accumulator pressure setpoint was reached, and the recovery process began.

The depletion of coolant mass in the vessel during Test S-UT-6 is depicted in Figure 1 which shows the collapsed liquid level (as measured with differential pressure cells) between the cold leg elevation and the bottom of the core. The minimum level measured in S-UT-6 during the loop seal depression was equivalent to the elevation of the bottom of the loop seals (approximately 220 cm above the bottom of the core heated length). A direct manometric balance of hydrostatic heads in the vessel and downflow side of the loop seals was established. The coolant mass distribution at 210 s (just prior to loop seal blowout) is depicted in Figure 2. The intact loop pump suction downflow side collapsed level was at the bottom of the loop seal and the vessel level was depressed to a corresponding elevation. The differential pressure through the broken loop was sustained in part by a column of liquid in the steam generator U-tubes. This type of PCS mass depletion and distribution is typical of previous Semiscale small break transient experiments.^{7,8}

The observed vessel hydraulic response during Test S-UT-8 was significantly more severe, in terms of vessel coolant depletion. The measured vessel collapsed liquid level for S-UT-8 is shown in comparison to the same measurement from S-UT-6 in Figure 1. A similar response is shown through 120 s after rupture; however, the level depression from pump suction liquid seal formation was much more rapid in S-UT-8, and continued far below the elevation of the bottom of the loop seals. Before the intact loop liquid seal was cleared at 240 s, the vessel level had been depressed to the bottom of the heated length of the core.

The hydraulic response observed during Test S-UT-8 was incongruous with the manometric balance behavior observed in previous Semiscale small break LOCA experiments. For the vessel level to be depressed below the

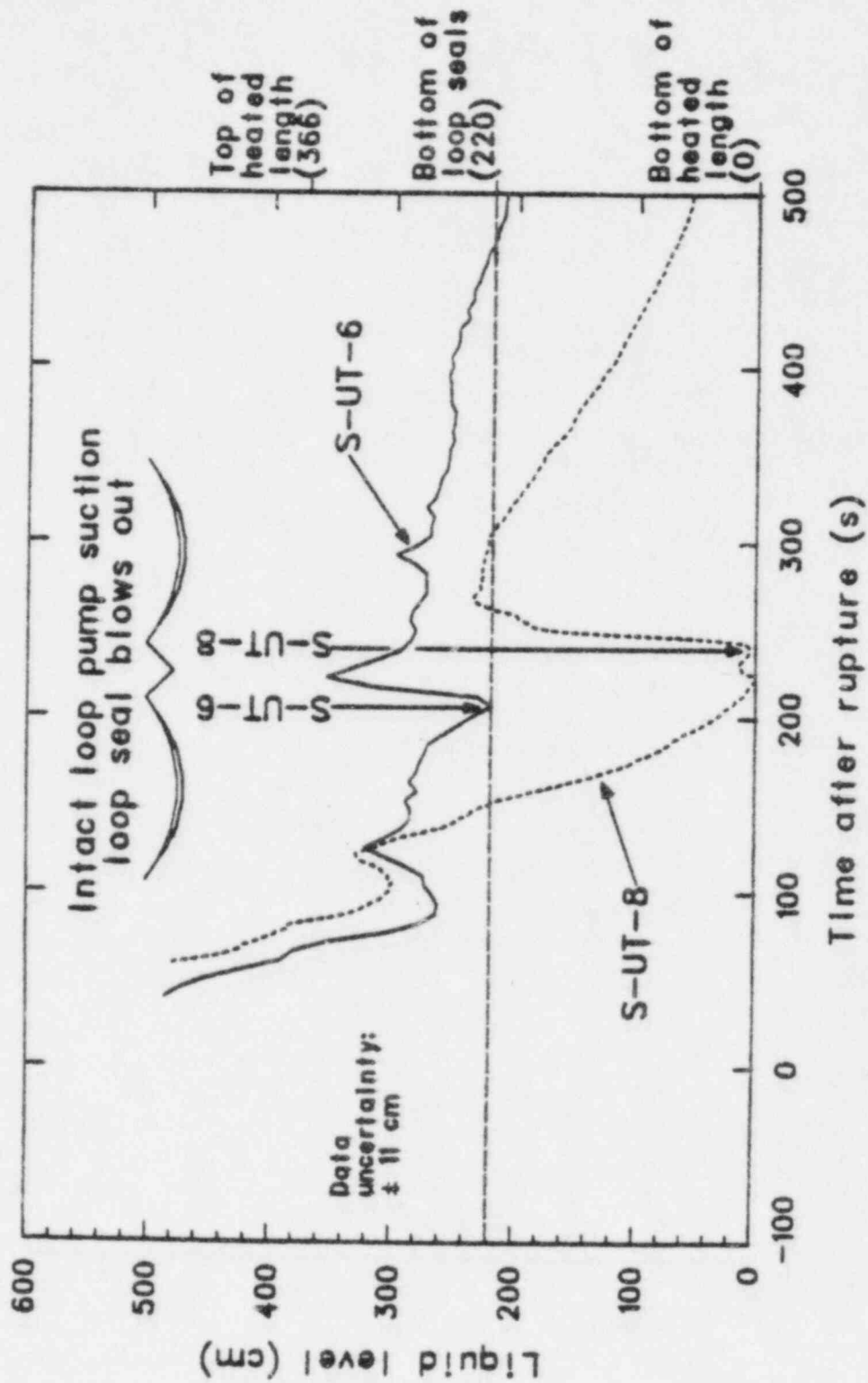


Figure 1. Vessel collapsed liquid level above the bottom of the core heated length.

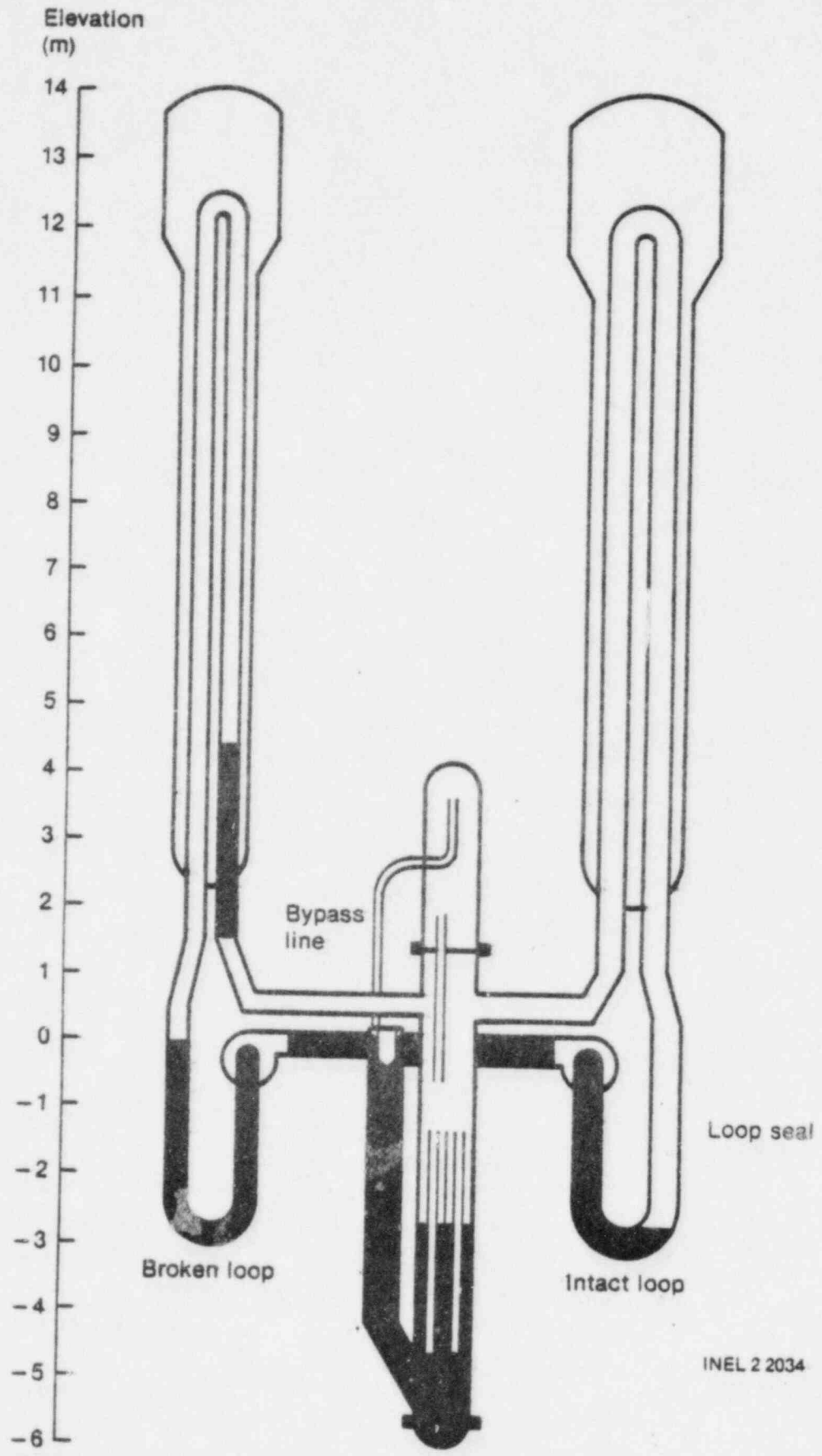


Figure 2. PCS mass distribution at 210 s after rupture (S-UT-6).

bottom of the loop seals, a significant change in the hot leg to cold leg differential pressure was required prior to loop seal clearing. The measured intact loop steam generator differential pressure (between the inlet and outlet plena) is shown for both experiments in Figure 3. A significant difference is shown between the two tests. The differential pressure in Test S-UT-6 diminished to approximately zero, 60 s prior to loop seal blowout. In Test S-UT-8, however, a differential pressure of 15.1 kPa remained at 210 s after rupture (when the intact loop liquid seal had already cleared in S-UT-6). This differential pressure is equivalent to 220 cm of hydrostatic head.

The differential pressure "rise" shown in each curve in Figure 3 after 50 s represents the difference in the hydrostatic heads of both sides of the steam generator U-tubes. Based upon separate liquid level measurements (with differential pressure cells) on the upflow and downflow sides of the intact loop U-tubes, the 15.1 kPa differential pressure at 210 s in S-UT-8 was caused by differences in hydrostatic heads. Figure 4 shows the intact loop U-tube upflow side liquid level measurement for both tests. The coolant level for Test S-UT-6, just prior to loop seal clearing, was nil. A delay in the U-tube drainage period is shown for S-UT-8 (as indicated in Figure 3), and a 220 cm level was measured at 210 s.

The PCS mass distribution at 210 s after rupture for Test S-UT-8 is depicted in Figure 5. A comparison of Figure 5 and Figure 2 provides a clear picture of the cause of the dramatic difference in the vessel hydraulic response shown in Figure 1. The remainder of this report provides a more detailed analysis of the reasons such a different response occurred and attempts to generalize the observed phenomenon through analysis of a full-scale PWR, utilizing the RELAP5 computer code.

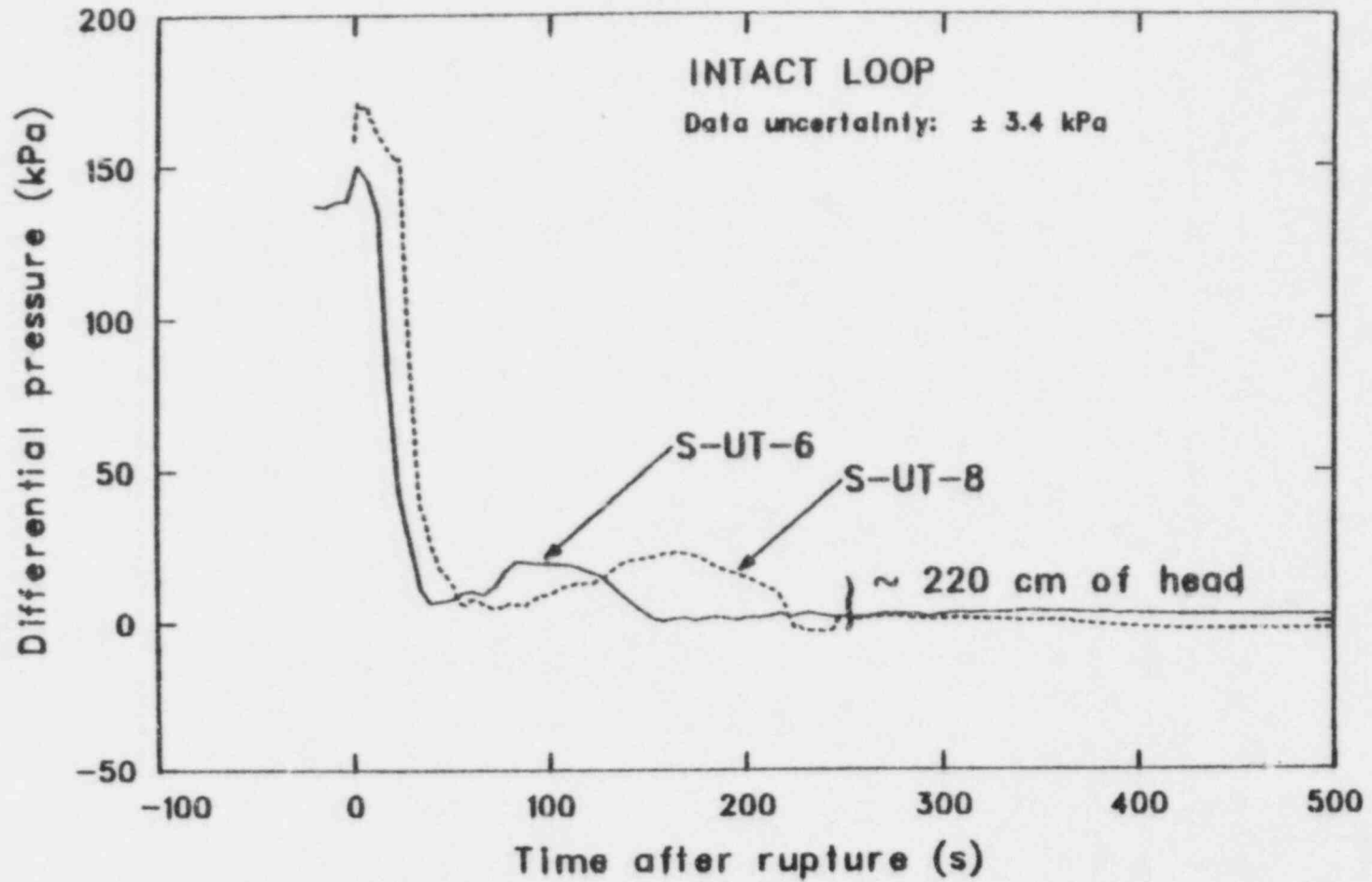


Figure 3. Intact loop steam generator primary side differential pressure.

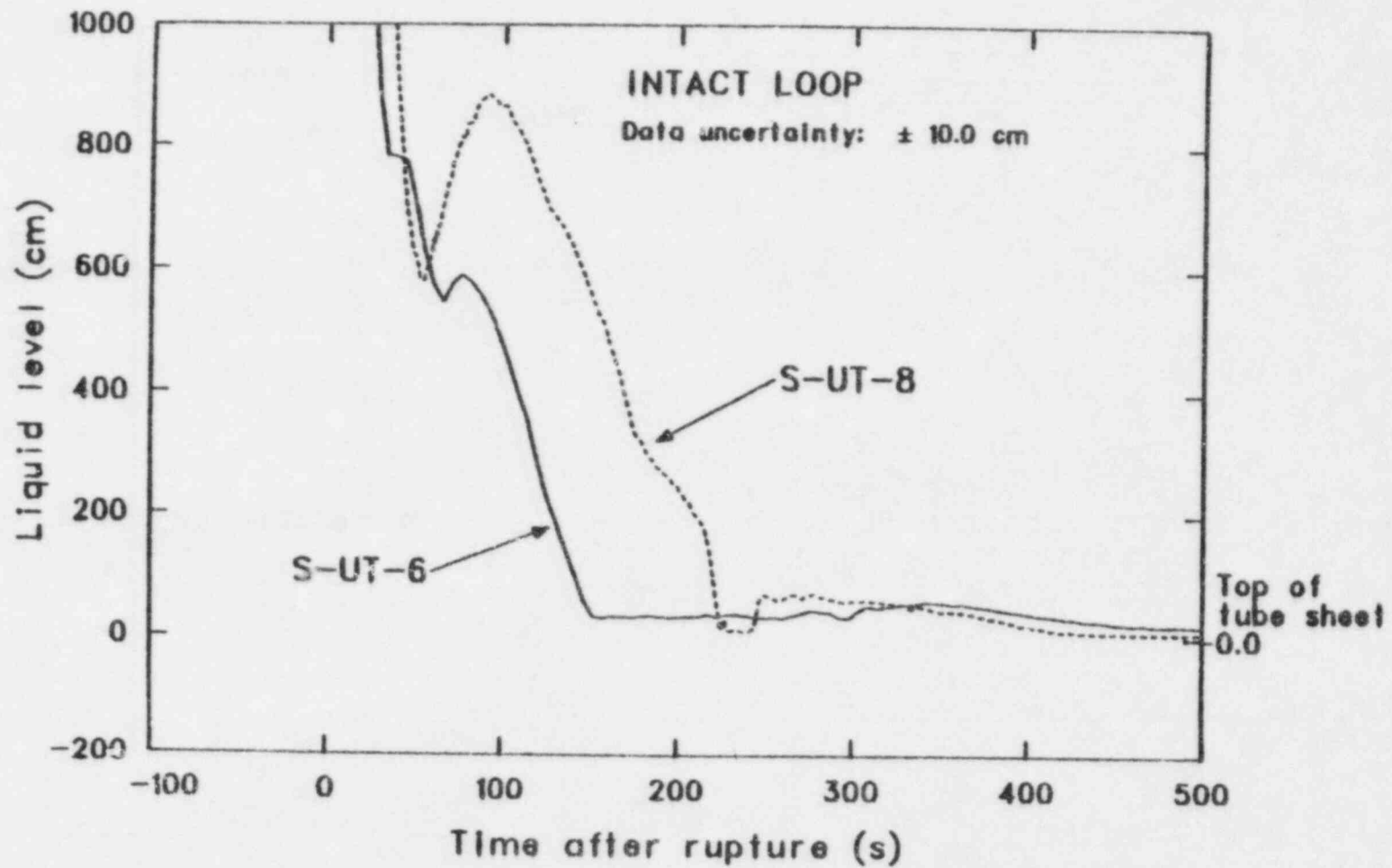


Figure 4. Intact loop steam generator U-tube upflow side collapsed liquid level.

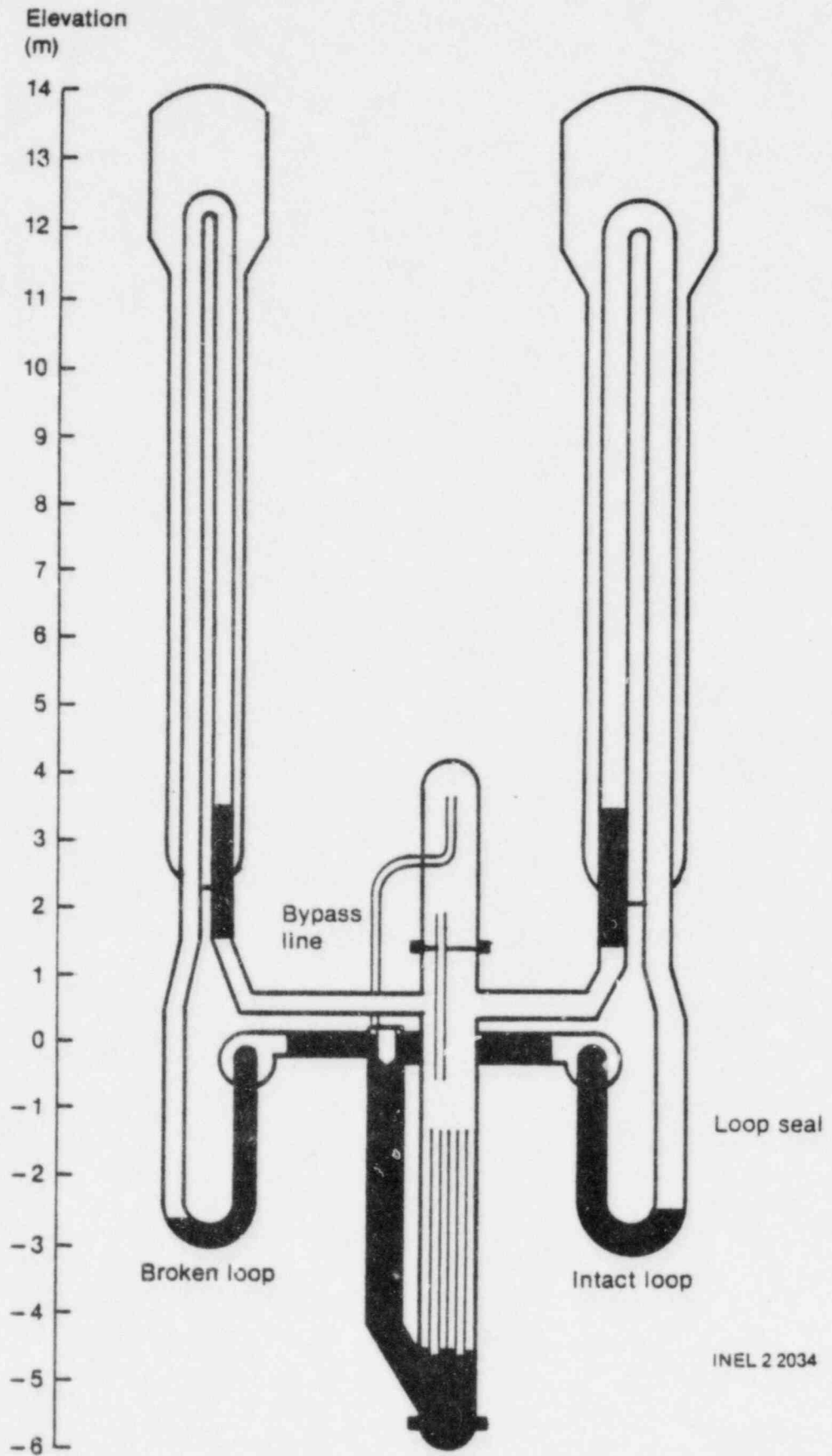


Figure 5. PCS mass distribution at 210 s after rupture (S-UT-8).

3. EXPERIMENTAL ANALYSIS

The primary objective of the analysis of Test S-UT-8 was to determine the cause of the extensive core voiding, observed during pump suction liquid seal formation. The discussion in Section 2 characterized this phenomenon in terms of the observed system transient conditions (PCS coolant distribution) required to depress the core level below the bottom of the loop seals. The following discussion presents a more detailed analysis of the specific hydraulic phenomena which induced the change in the system coolant distribution prior to loop seal blowout.

The conclusion drawn from this analysis is, that a reduction in the bypass flow rate^a and differences in the intact loop steam generator secondary operating conditions between Tests S-UT-6 and S-UT-8 were the causes of the increased U-tube hydrostatic head during pump suction liquid seal formation.

A comparison of the system hardware configuration and experimental data between the two Semiscale tests revealed four hypothetical causes of the different hydraulic responses: initial conditions, transient operations, vessel upper head modifications, and core bypass flow rate. Each of these hypothetical causes was evaluated with the existing experimental data. When sufficient data were not available to evaluate the feasibility of a hypothetical cause, analytical modeling was applied to estimate the potential of the cause.

3.1 Initial Conditions

The primary and secondary fluid initial conditions for both experiments are compared in Table 1. With the exception of the bypass

a. "Bypass" flow is used here to mean any flow path between the cold leg inlet to the vessel downcomer and the vessel upper plenum without penetrating the downcomer. In these experiments, the bypass path was through the upper head.

TABLE 1. EXPERIMENTAL INITIAL CONDITIONS

	S-UT-6	S-UT-8	Data Uncertainty
Upper plenum pressure (MPa)	15.81	15.57	+0.054
Cold leg temperature (K)			
Intact loop	557.	559.	+2.0
Broken loop	557.	561.	+2.0
Core ΔT (K)	42.0	39.5	+2.8
Core outlet flow rate (L/s)	13.5	14.4	+0.7
Bypass flow (%)	4.0	1.5	+1.0
Steam generator secondary pressure (MPa)			
Intact loop	5.7	5.72	+0.03
Broken loop	5.9	6.08	+0.03
Steam line fluid temperature (K)			
Intact loop	545.	546.	+2.0
Broken loop	548.	549.	+2.0
Total secondary coolant mass ^a (Kg)			
Intact loop	150.	190.	+20.0
Broken loop	60.	170.	+20.0

a. Values estimated from measured secondary level after steam and feedwater line isolation.

flow, steam generator secondary coolant mass is the only parameter shown to differ substantially beyond the range of data uncertainty. Typically, the effect of secondary coolant mass on a small break LOCA is to influence the pressure at which the primary and secondary coolant systems approach equilibrium. Higher secondary coolant masses have been observed to result in higher peak secondary pressures at steam generator isolation and a slower rate of pressure decay thereafter. This trend is understandable since more coolant mass implies less volume into which the confined vapor produced can expand. The important question, is whether the resulting higher secondary coolant pressures (and temperatures) in Test S-UT-8 played a role in increasing the U-tube hydrostatic head relative to that observed in S-UT-6. The measured secondary coolant levels and steam dome pressures are shown in Figures 6 and 7, for the intact and broken loop, respectively.

A higher PCS pressure was measured in Test S-UT-8 than S-UT-6 as the PCS approached equilibrium with the intact loop secondary. Figure 8 shows the upper plenum pressure for both experiments. The measured difference in upper plenum pressure, shown between 20 and 220 s, represents a small difference in PCS thermodynamic conditions, however.

The effects of steam generator secondary coolant conditions on pump suction liquid seal dynamics are not entirely understood. Some evidence that loop seal blowout is influenced by the thermodynamic conditions of the secondary coolant relative to those of the primary coolant have been documented.⁹ The suggested effect is that condensation in the U-tubes reduces the net vapor mass flux into the downflow side of the pump suction loop seal. A Nusselt analysis (detailed in Appendix B) for the intact loop steam generator U-tubes predicts that a 3 K temperature differential, between the primary and secondary fluids is required to condense the maximum potential vapor mass flux (at 3.1% of full core power and 6.9 MPa PCS pressure^a) on half the surface area of the U-tubes. A more elaborate condensation model by Carpenter and Colburn¹⁰ predicts a minimum

a. Typical conditions during liquid seal formation.

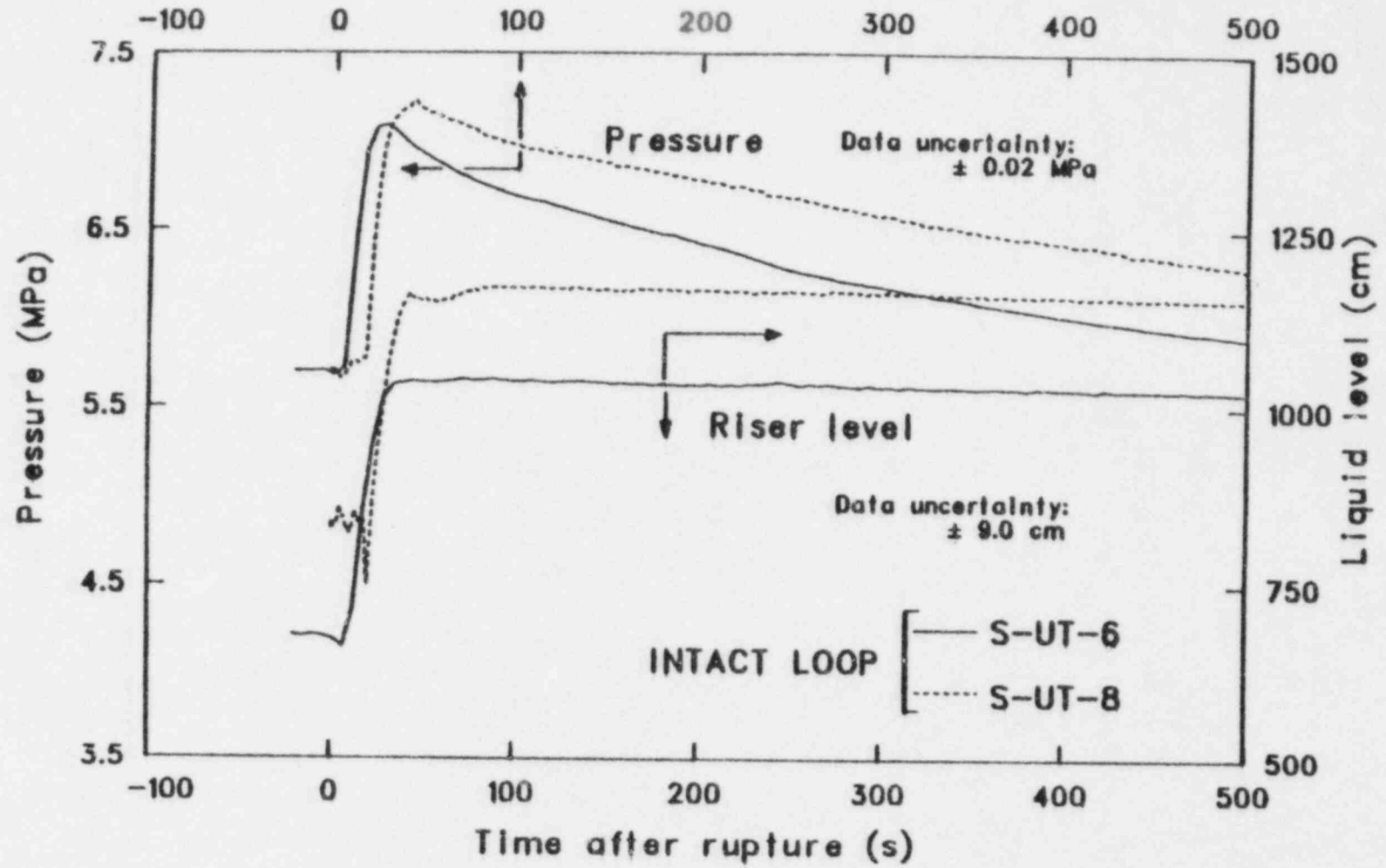


Figure 6. Intact loop steam generator secondary coolant conditions.

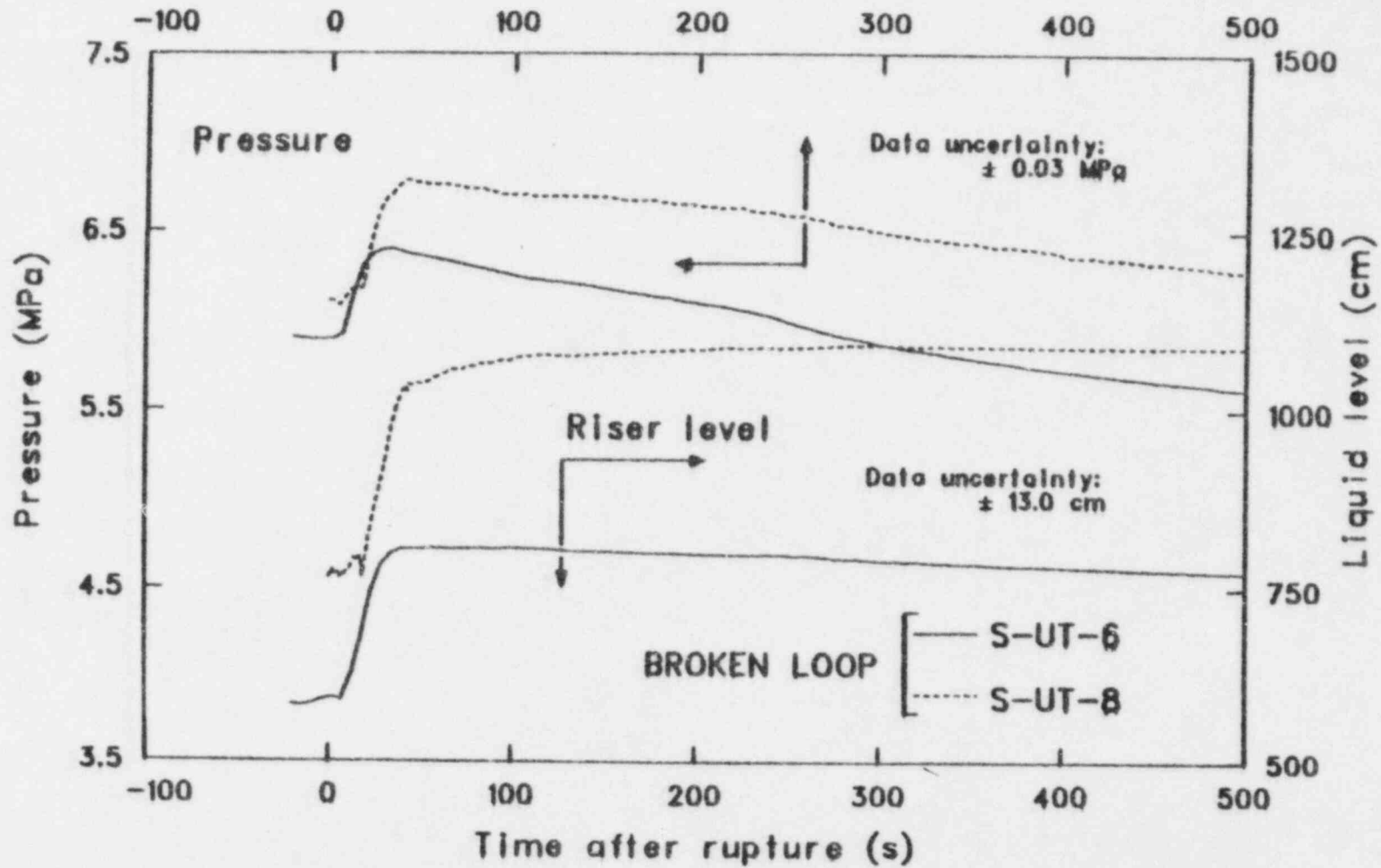


Figure 7. Broken loop steam generator secondary coolant conditions.

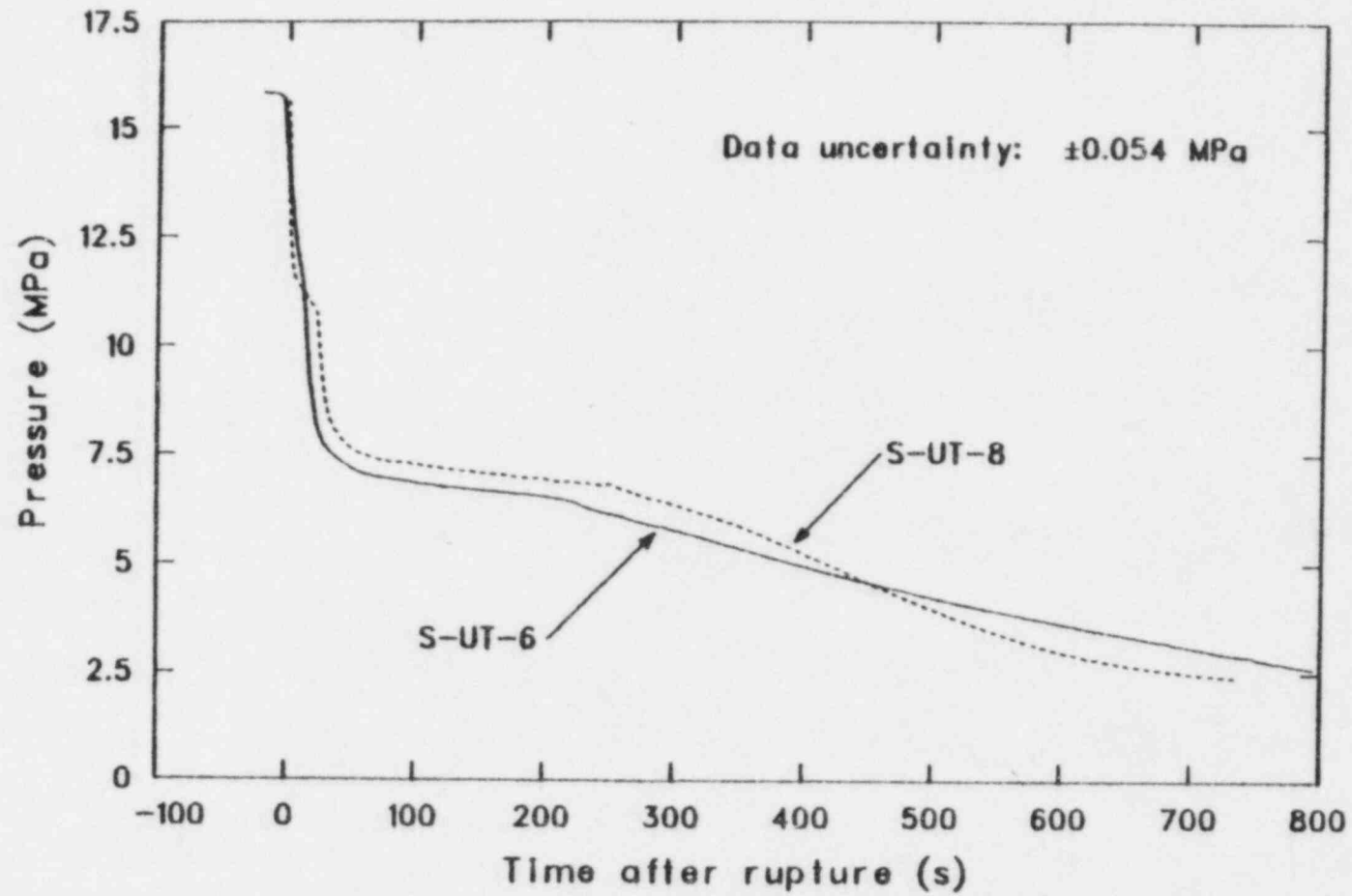


Figure 8. Vessel upper plenum pressures.

temperature differential of 13 K (Appendix B). The latter model result is probably closer to reality since turbulent conditions are possible on the vapor/condensate interface and the Colburn model considers the effects of interfacial shear on film condensation.

Figure 9 shows the measured fluid differential temperature^a between the primary and secondary coolant in the upflow side of the intact loop steam generator U-tubes (30 cm above the top of the tube sheet) for both experiments. A sufficient condensation potential (i.e., to condense the maximum steam flow) is seen to exist for the first 70 s of Test S-UT-6 and 100 s of Test S-UT-8. During these time periods the upflow side of the U-tubes were calculated to be flooded^b (see Appendix C) and the collapsed liquid levels in both the upflow and downflow sides increased, as shown in Figure 10 for Test S-UT-8. (Note that equal condensation potential exists on both sides of the tubes.) In both tests, the increase in liquid levels ceases when the primary and secondary temperatures near equilibration, at which time the condensation potential is lost.

The significant difference between the two tests lies in the length of time during which the condensation could take place. In Test S-UT-8, this period was at least 30 seconds longer, thereby delaying the time at which drainage of the U-tubes could begin.

As shown in Figure 10, the upflow side collapsed liquid level always exceeds that in the downflow side (this was true for both experiments). This difference is what gives rise to a net positive hydrostatic head across the steam generator prior to loop seal clearing. The fact that there was a longer period of condensation potential in S-UT-8 resulted in the shift in time of the buildup and decline in the steam generator ΔP (Figure 3). In

a. The primary and secondary fluid temperatures were measured independently and differenced in data processing.

b. Flooding as used here means a situation in which the rising vapor mass flux is at least as large as the descending liquid mass flux.

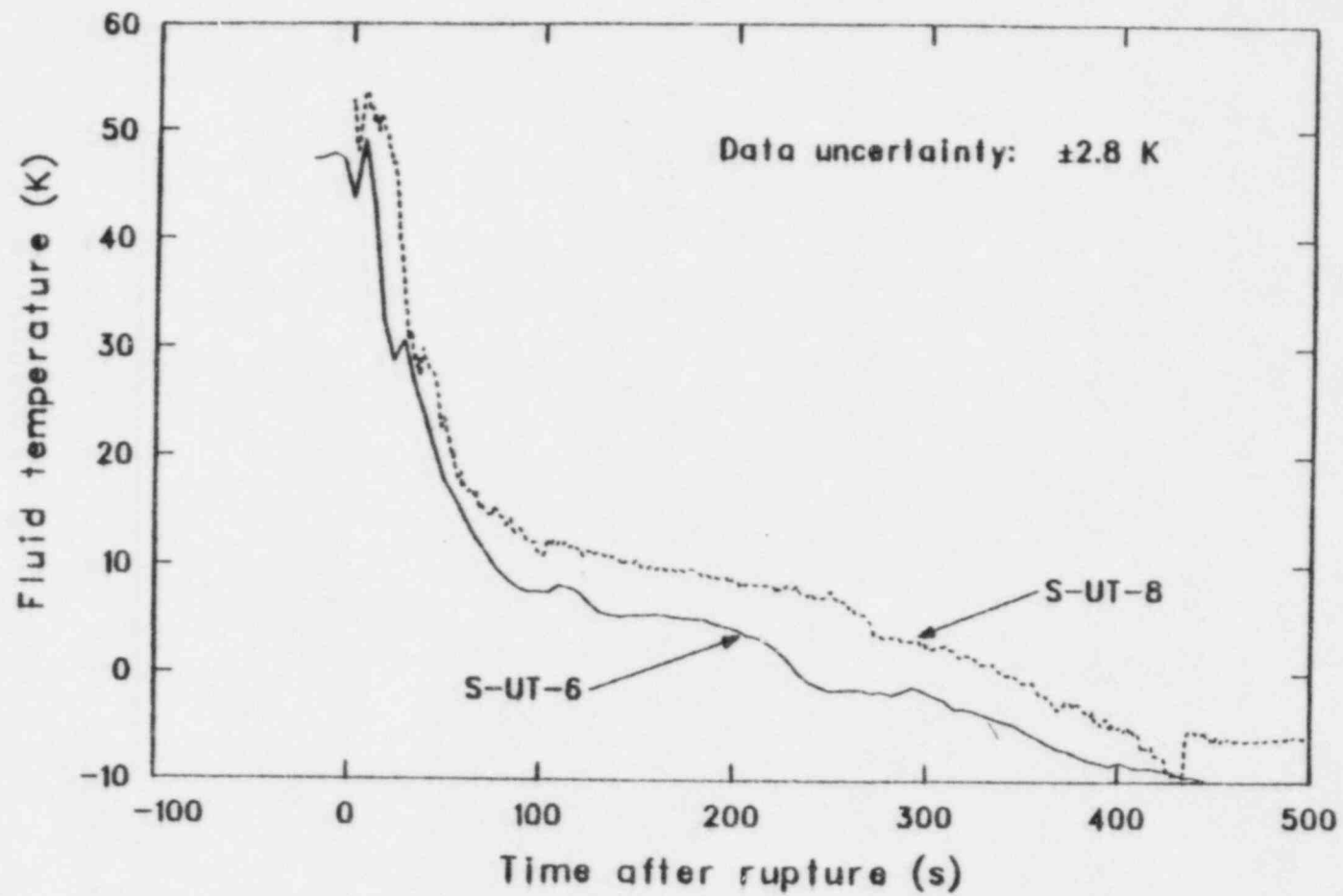
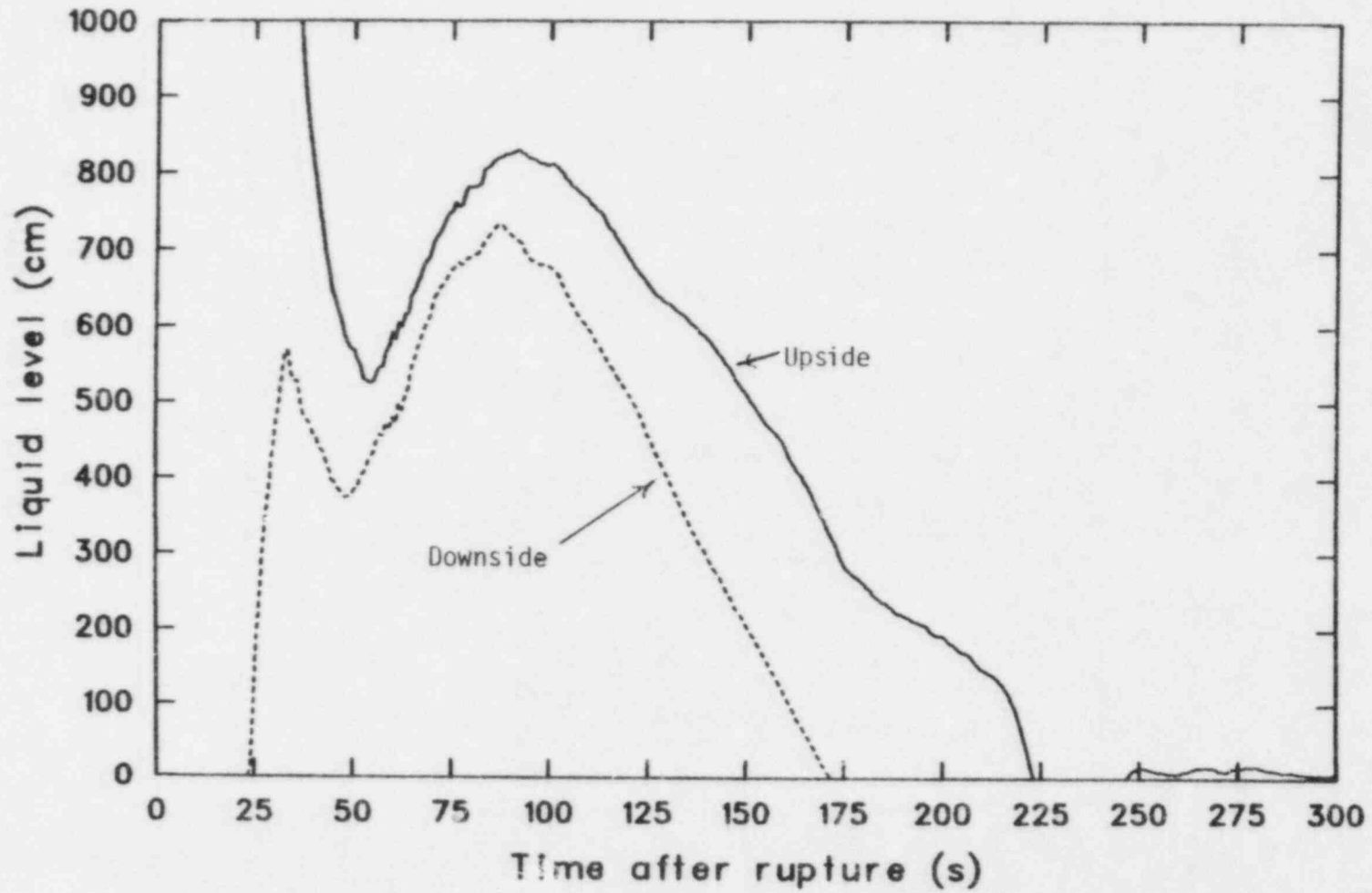


Figure 9. Primary/secondary fluid differential temperature (30 cm above tube sheet - upflow side).



WRTF23-2

Figure 10. Intact loop steam generator U-tube upflow side collapsed liquid level.

Test S-UT-6, the U-tube hydrostatic head had diminished to zero by 150 s, approximately 60 s prior to loop seal clearing. In contrast, the hydrostatic head at loop seal clearing in S-UT-8 was 220 cm.

3.2 Transient Operational Differences

The time at which core power and the PCS pumps were tripped in the two experiments was different by approximately 8 s. Both trips were initiated by a low pressurizer pressure signal at approximately 12.6 MPa, with a 3.4 s time delay. The low pressure signal was received approximately 8 s later in Test S-UT-8 than in S-UT-6. In both experiments, the normalized core power and pump speed decay curve were approximately the same; only the time of trip was different.

The delay in the core power and PCS pump trip in S-UT-8, relative to S-UT-6 resulted from a significant difference in the pressurizer surge line hydraulic resistance. The surge line resistance was calculated^a to have been approximately 10^9 m^{-4} in Test S-UT-6 and 10^{10} m^{-4} in Test S-UT-8. The effect of the different surge line resistance was to lengthen the pressurizer drainage period from 10 s in S-UT-6 to 20 s in S-UT-8. Concurrently, the lag of the pressurizer pressure, behind the hot leg pressure, was exaggerated in Test S-UT-8 as shown in Figure 11. The time at which the 12.6 MPa pressure setpoint was reached was, therefore, delayed.

An additional eight seconds of full core power were applied in Test S-UT-8 compared to S-UT-6. The PCS pump trips were also delayed, as were the steam line and feedwater isolation in the steam generator secondaries. The overall effect was, therefore, not significant in terms of the long-term transient response of the system, since the total system energy balance was not distorted, only shifted in time.

a. The Δp between the pressurizer and hot leg was measured and the pressurizer flow rate may be calculated by integrating the measured liquid level ($R' = \Delta p \rho / \mu^2$) [m^{-4}].

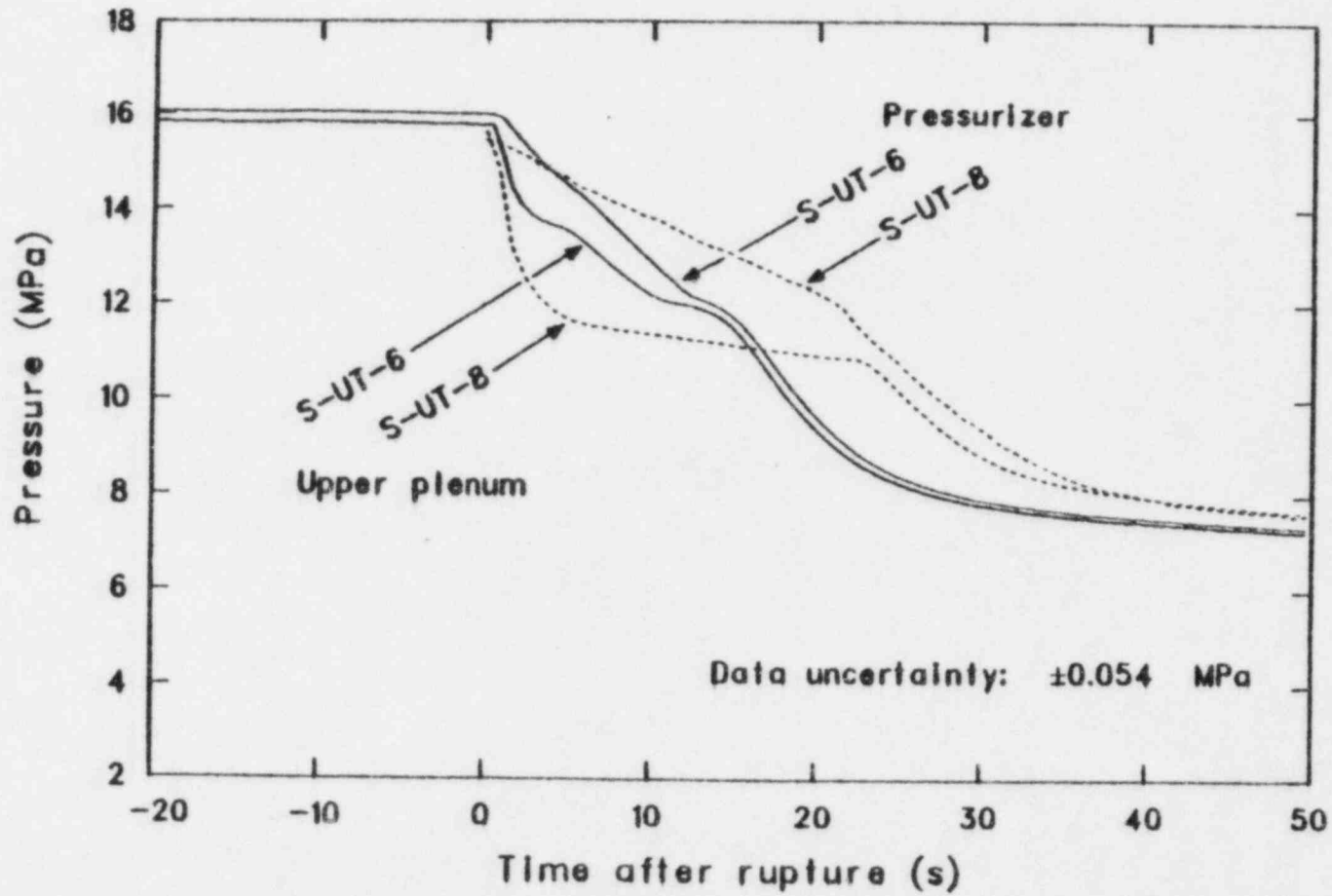


Figure 11. Pressurizer and upper plenum pressures.

3.3 Vessel Upper Head Modifications

As described in Appendix A, modifications to the vessel upper head configuration were made between Tests S-UT-6 and S-UT-8. The modifications were intended to enhance the typicality of the Mod-2A vessel upper head drainage characteristics. During the initial data review, following Test S-UT-8, it was observed that a relatively large leakage path between the upper head and upper plenum had not been sealed. This path did not alter the ability to fix the total bypass flow resistance since it was adjusted on-line with a valve in the bypass line (connecting the downcomer inlet annulus to the upper head). Upon transient initiation, the upper head drain rate was impacted, however.

The collapsed liquid level in the vessel upper head (measured with differential pressure cells) is shown for both experiments in Figure 12. The upper head is shown to empty significantly earlier in Test S-UT-8 than in Test S-UT-6. Since the location of the extra drainage path is known, it is reasonable to assume that the major portion of the upper head fluid drained into the vessel upper plenum in Test S-UT-8. (The guide tube hydraulic resistance was designed to be only 9.3% of the bypass line resistance.⁵) Further, the amount of upper head fluid which drained to the upper plenum, rather than the cold legs (via the bypass line), was probably less in Test S-UT-6 than in S-UT-8. This cannot be verified, since a bypass line flow measurement was not available for Test S-UT-8. However, the guide tube hydraulic resistance (relative to the bypass line) was higher in Test S-UT-6 than S-UT-8, and the total support column flow area (open for S-UT-6 but not for S-UT-8) was slightly smaller than the estimated S-UT-8 leakage area. The differences in upper head configuration between the two experiments did not, therefore, impede the delivery of fluid from the upper head to the upper plenum.

Provided that upper head fluid, falling through the upper plenum, was not entrained and swept into the hot legs as a result of the more rapid drain rate in Test S-UT-8, the total amount of coolant delivered to the core was approximately equivalent in both tests. No entrainment beyond that possible during Test S-UT-6 is indicated in the S-UT-8 intact loop hot

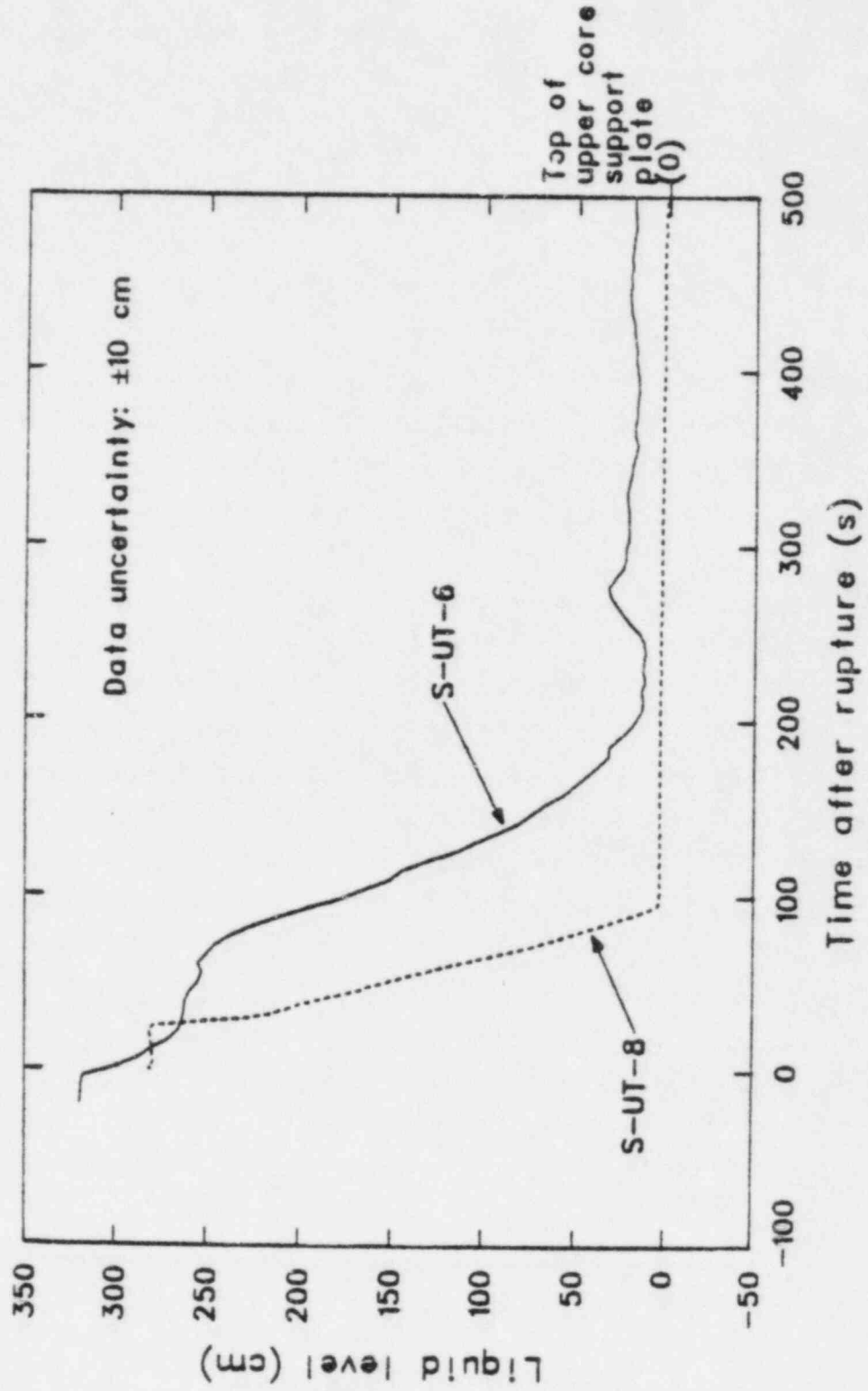


Figure 12. Vessel upper head collapsed liquid level.

leg data. The measured volumetric flow rate and average chordal densities in the intact loop hot leg are shown for the two experiments in Figures 13 and 14, respectively. No significant difference is shown between the experimental measurements, apart from the temporal shift in Figure 13 due to the delayed pump trip in S-UT-8.

3.4 Bypass Flow Rate Effect

The effect of decreasing the core bypass flow in Test S-UT-8 relative to that in S-UT-6 was to increase the flow of steam from the vessel to the hot legs prior to loop seal clearing. This follows from the fact that the flow path between the top of the vessel and the downcomer had been made more restrictive, thus diminishing the ability of steam to flow directly from the vessel to the cold leg, bypassing the steam generator and pump.

During the time that a substantial condensation potential existed in the intact loop steam generator in both tests, the hot leg steam flow was sufficiently high to prevent drainage of the upside of the U-tubes (see Appendix C). In both tests, once the condensation potential had diminished the steam velocities were not high enough to prevent drainage, but did retard the rate of drainage. To the extent that the steam velocities were greater in Test S-UT-8, the drainage rate of the upflow side of the U-tubes was further retarded over that in Test S-UT-6. This difference in drainage rates, shown in Figure 15, accentuated the difference in positive hydrostatic head in the two experiments prior to loop seal clearing. Thus, while the difference in bypass flow between the two experiments was not entirely responsible for the deeper core uncover observed in Test S-UT-8, it was a significant contributing factor.

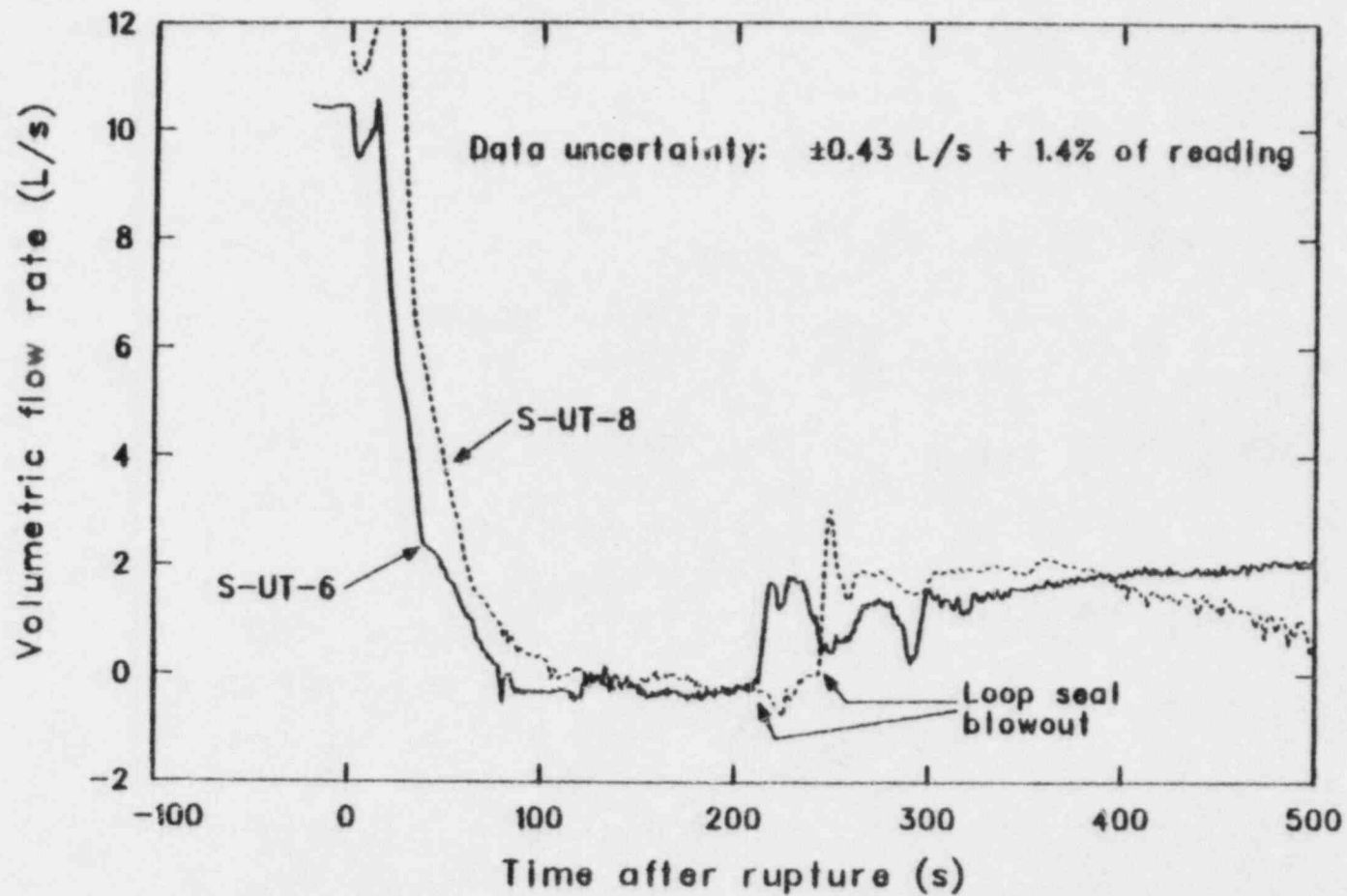


Figure 13. Intact loop hot leg volumetric flow rate.

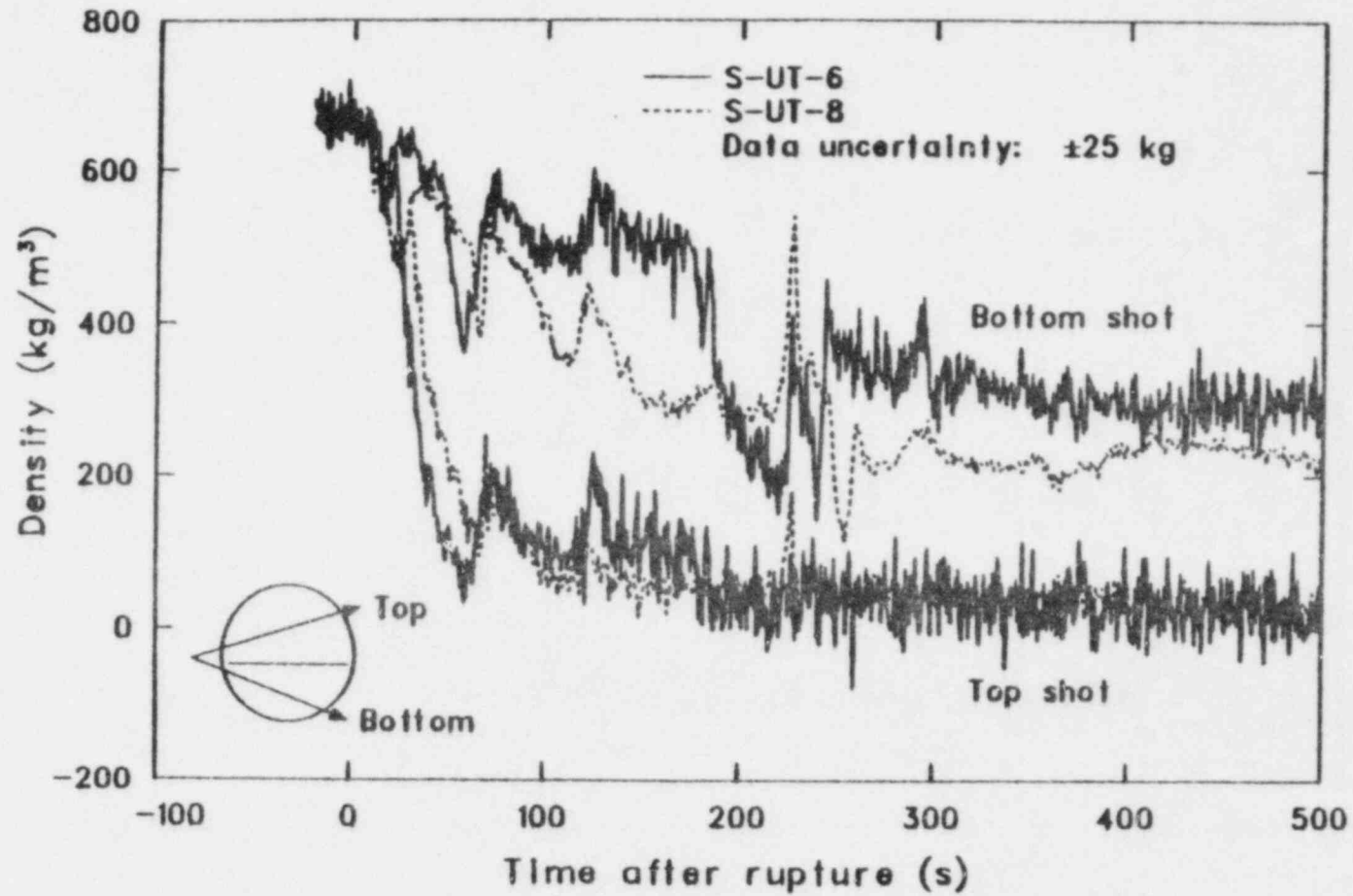


Figure 14. Intact loop hot leg average chordal densities.

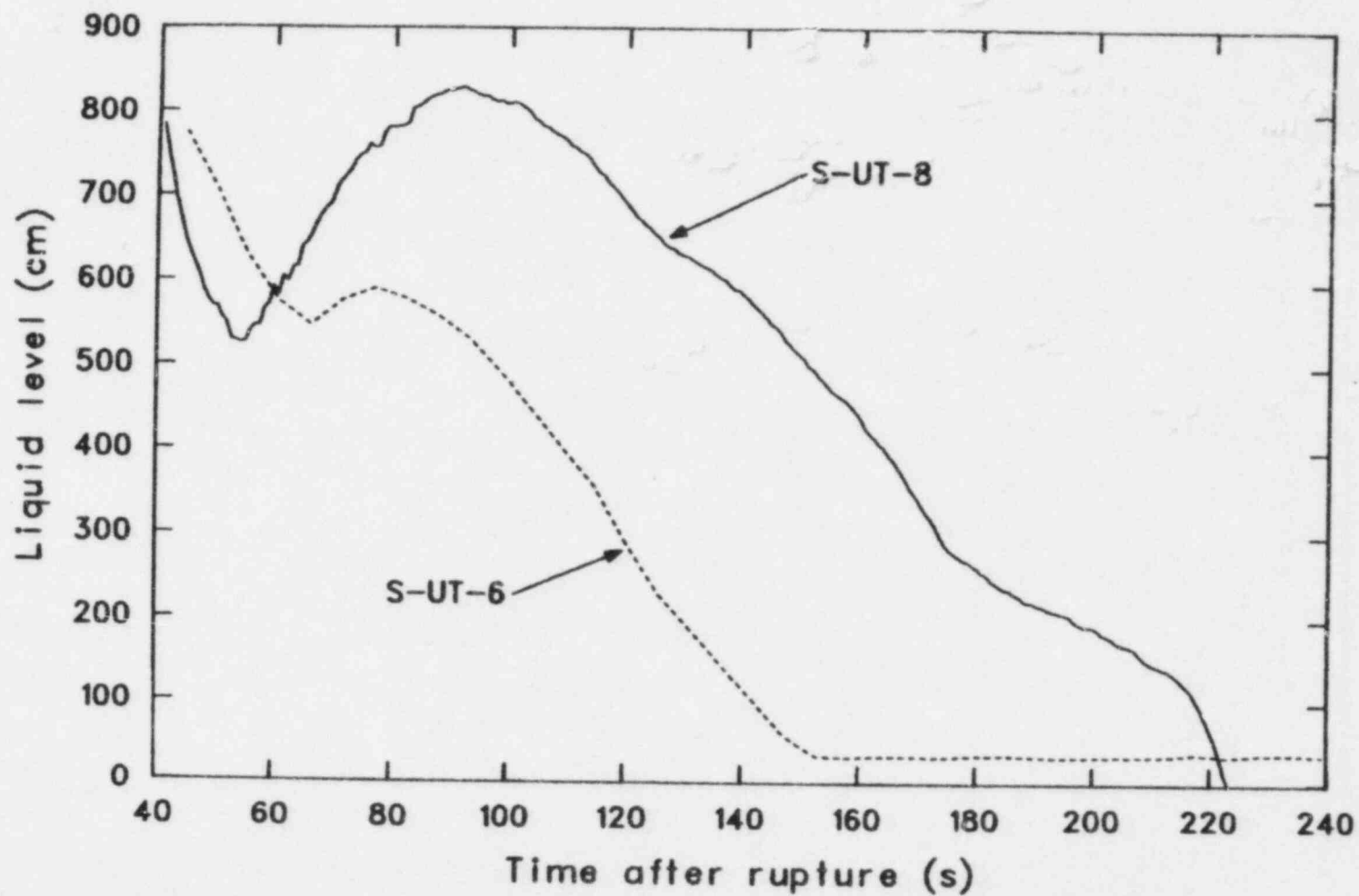


Figure 15. Comparison of measured intact loop steam generator upflow-side U-tube collapsed liquid levels for Tests S-UT-6 and S-UT-8.

4. GENERALIZED PHENOMENOLOGICAL ANALYSIS

The analysis of experimental data from Tests S-UT-6 and S-UT-8 suggested a correlation might exist between PCS bypass flow and vessel coolant mass depletion. The number of data points available to generalize the phenomenon is small, however (including other Semiscale small break data, three break sizes with 4.0% bypass and one break size with 1.5% bypass). As a method of expanding the "data" base, a best-estimate computer code was applied to a typical full-scale PWR system model to calculate several small break transients for several values of bypass flow.

The RELAP5/MOD1¹² computer code was used for the small break/bypass analysis. The code has previously demonstrated the capability of calculating the overall thermal-hydraulic response of small break experiments in the Semiscale facility.² To ensure the code's capability to calculate the change in thermal-hydraulic response observed in Test S-UT-8 from Test S-UT-6, a calculation of each experiment was performed. The RELAP5 model used for these calculations is documented in Reference 3.

The calculated vessel hydraulic response, as represented by the collapsed liquid level above the bottom of the core heated length, is shown in comparison to the corresponding data for the two experiments in Figure 16. For both experiments, the minimum collapsed level during pump suction liquid seal depression was calculated in good agreement with the data. The calculated recovery of the vessel level following loop seal clearing did not agree with the measured response. However, for the purpose of this analysis, the code demonstrated the capability of calculating the difference in the vessel coolant mass depletion during liquid seal formation between the two experiments.

A RELAP5 model very similar to that used for the Semiscale calculations, but developed for a full-scale PWR, was used to characterize the phenomenon over a range of bypass flow rates and break sizes. The nodalization scheme for the upper portion of the reactor vessel is shown in Figure 17. The bypass flow path from the cold leg, up through the upper

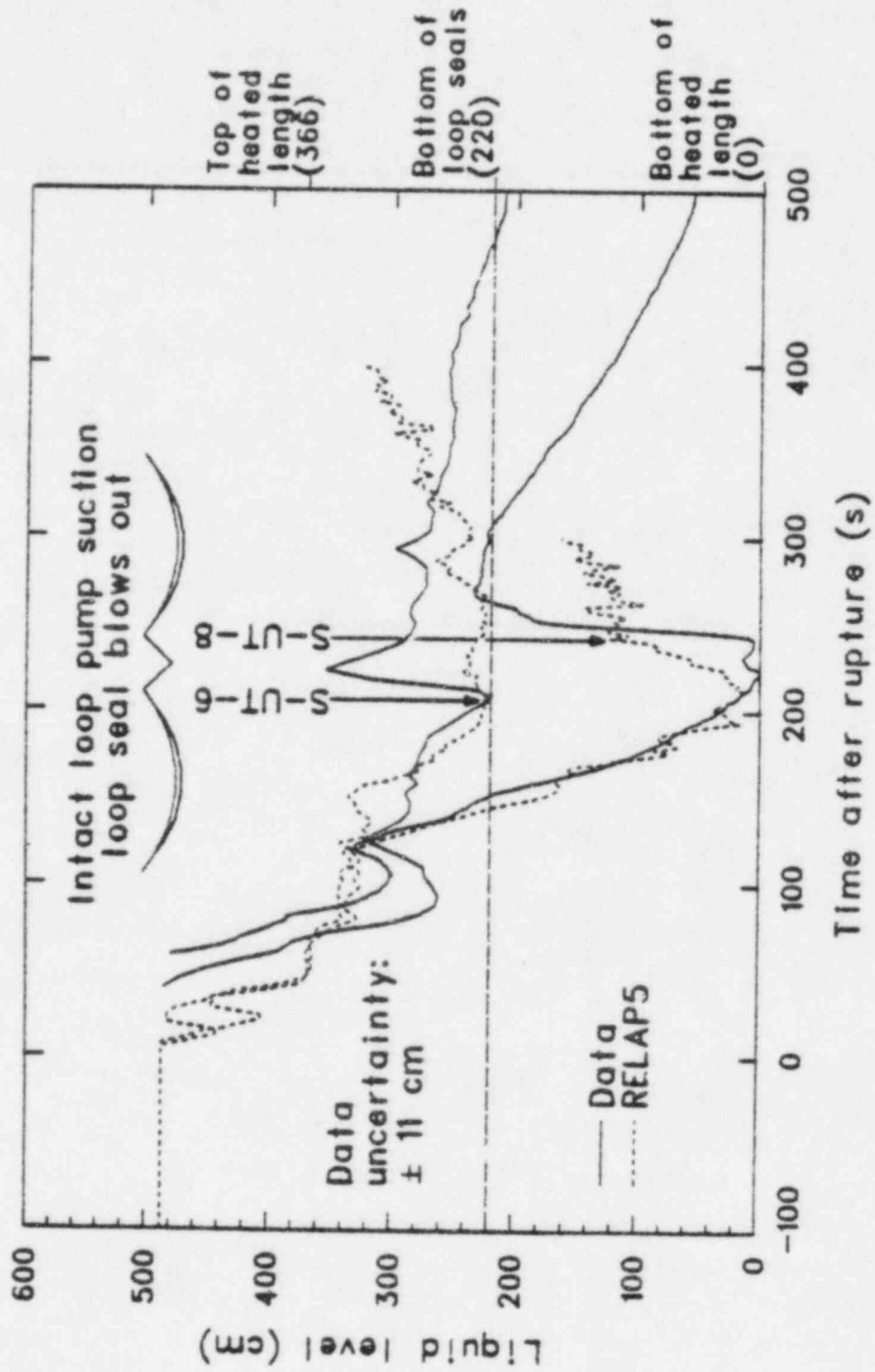


Figure 16. Measured and calculated vessel collapsed liquid level (Tests S-UT-6 and S-UT-8).

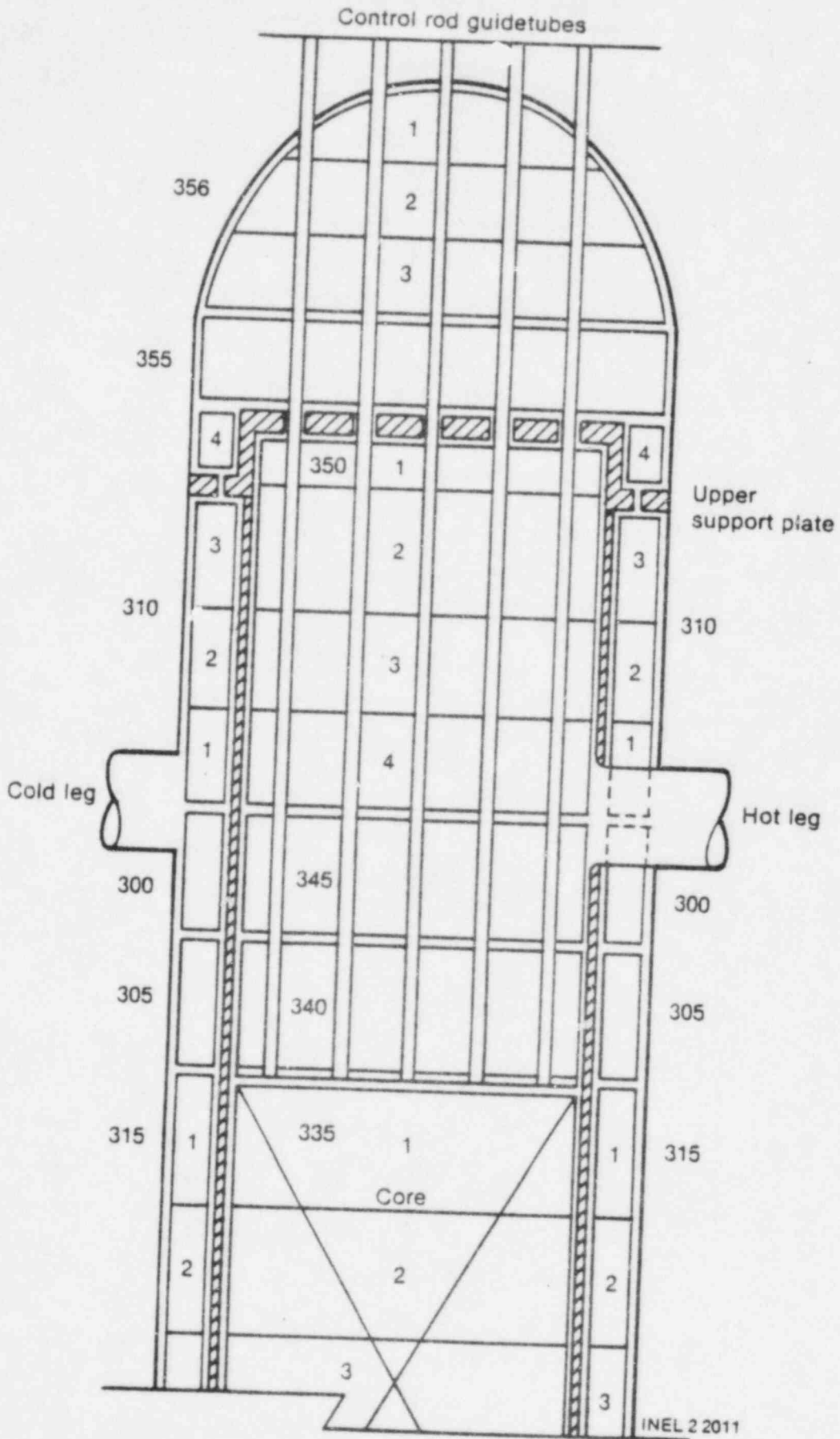


Figure 17. PWR RELAP5 reactor vessel nodalization.

core support plate to the upper head is illustrated. A return flow path to the upper plenum is shown around the control guide tube housings in the upper core support plate.

The PWR calculated results are summarized in Figure 18 which shows the minimum core collapsed level during pump suction liquid seal formation,^a for three values of bypass flow over a range of break sizes. Among all of these calculations, the only difference in the RELAP5 system model used was the specified hydraulic resistance (in terms of flow head) through the bypass flow path. The calculated results are also shown in comparison to Semiscale data.^{6,7,8}

For the break size simulated in Experiments S-UT-6 and S-UT-8 (5.0%), an abrupt change in the degree of coolant mass depletion is predicted for the PWR model below 4.0% bypass. The upper and lower bounds of the calculated results (4.0 and 2.0% bypass) are shown to be in good agreement with the Semiscale data at approximately the same bypass rates. (This result is similar to that shown in Figure 16). For the other break sizes, a similar trend is shown (increased vessel coolant mass depletion with decreasing bypass), but the change in the calculated minimum level is less dramatic than that shown for the 5.0% break size.

a. Minimum level prior to loop seal clearing.

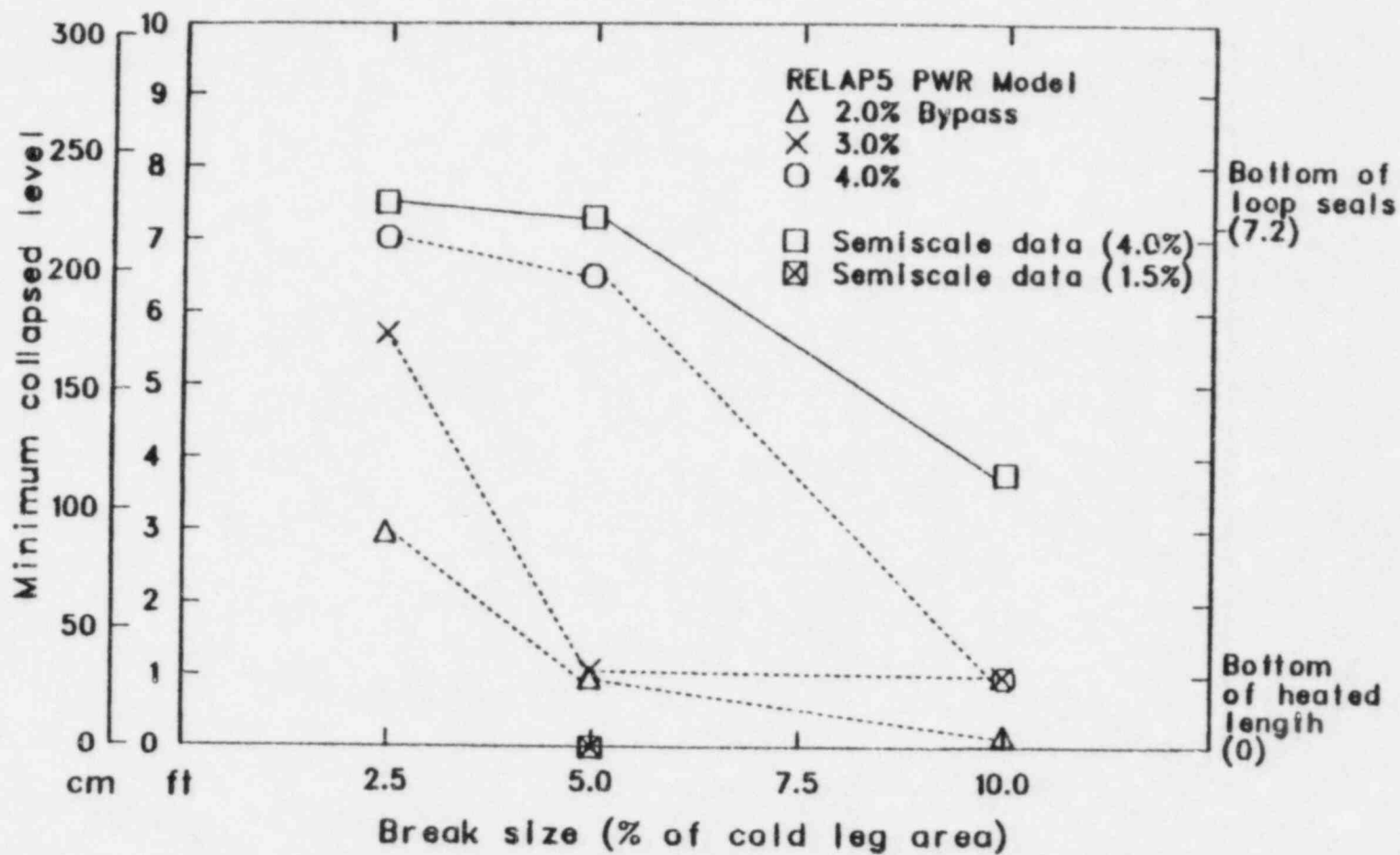


Figure 18. Minimum core collapsed liquid level during pump suction liquid seal formation.

5. CONCLUSIONS

A posttest analysis has been performed for a pair of small break LOCA experiments in a scaled, integral PWR facility. The experimental results have identified an unanticipated hydraulic phenomenon during the period which is typically characterized by the depression of the core coolant level in the reactor vessel, due to the formation of liquid seals in the primary coolant loop pump suction piping. The following specific conclusions have been drawn concerning the degree of core coolant level depression and the associated vessel coolant mass depletion during a small break LOCA.

1. The degree of core coolant level depression during pump suction liquid seal formation can be aggravated by the existence of a positive hydrostatic head in the steam generator U-tubes, due to the trapping of liquid in the upflow side of the tubes. This hydrostatic head increases the vessel to cold leg pressure differential, thereby increasing the corresponding manometric level difference between the vessel and downcomer. The maximum level difference can therefore exceed the elevation difference between the cold leg and pump suction U-bend.
2. The timing of the steam generator U-tube drainage relative to the clearing of the loop seal is important in that any mechanism that serves to delay drainage will act to magnify the differential pressure between the vessel and cold leg prior to loop seal clearing.
3. Coolant bypass flow and steam generator condensation potential can act in combination (exemplified in the Semiscale data) or individually (as seen in the PWR calculations) to influence the onset and rate of drainage of the steam generator U-tubes.

In summary, the effect of loop seal behavior on a small break LOCA has been shown to be more complex than a simple manometric balance between the reactor vessel and downflow leg of the loop seals. Several competing rate

processes combine to determine the primary coolant mass distribution prior to the blowout of the pump suction liquid seals. Core vapor generation, core coolant bypass, U-tube condensation, and flooding all have important roles in the determination of vessel coolant mass depletion. The significance of the results presented herein lies not so much in the incipient causes of steam generator U-tube liquid storage but rather that such storage can occur and will give rise to a dramatic difference in the vessel level behavior. Consequently, it is essential that analytical tools (i.e., computer codes) used to predict full-scale PWR behavior during small break LOCAs be capable of describing the thermal-hydraulic phenomena that can influence this liquid storage.

REFERENCES

1. R. J. Skwarek, "Experimental Evaluation of PWR Loop Seal Behavior During Small LOCAs," Small Break Loss-of-Coolant Accident Analyses in LWRs, Conference Papers, Specialists Meeting, Monterey, California, August 25-27, 1981, EPRI WS-81-201, pp. 5-1 to 5-11.
2. M. T. Leonard, Posttest RELAP5 Simulations of the Semiscale S-UT Series Experiments, EGG-SEMI-5622, EG&G Idaho, Inc., October 1981.
3. M. T. Leonard, RELAP5 Standard Model Description for the Semiscale Mod-2A System, EGG-SEMI-5692, EG&G Idaho, Inc., December 1981.
4. R. A. Larson, L. Bruce Clegg, Experiment Data Report for Semiscale Mod-2A Small Break Test Series (Test S-UT-6 and S-UT-7), NUREG/CR-2355, EGG-2132, November 1981.
5. W. W. Tingle, Experiment Operating Specification for Semiscale Mod-2A 5.0% Break Experiment S-UT-8, EGG-SEMI-5685, EG&G Idaho, Inc., December 1981.
6. J. M. Cozzuol, C. M. Kullberg, Quick Look Report for Semiscale Mod-2A Test S-UT-6, EGG-SEMI-5446, EG&G Idaho, Inc., May 1981.
7. K. E. Sackett, L. B. Clegg, Experimental Data Report for Semiscale Mod-2A Small Break Test Series (Tests S-UT-1 and S-UT-2), NUREG/CR-2176, EGG-2108, July 1981.
8. K. Sackett, L. B. Clegg, Experimental Data Report for Semiscale Mod-2A Small Break Test Series (Tests S-UT-4 and S-UT-5), NUREG/CR-2349, EGG-2131, November 1981.
9. T. J. Boucher, M. T. Leonard, Quick Look Report for Semiscale Intermediate Break Test S-13-3, EGG-SEMI-6013, EG&G Idaho, Inc., (To be Published).
10. E. F. Carpenter, A. P. Colburn, "The Effect of Vapor Velocity on Condensation Inside Tubes," Proc. of General Discussion on Heat Transfer, Inst. Mechanical Engineers/ASME, pp. 20-26, 1951.
11. G. B. Wallis, One-dimensional Two-phase Flow, New York: McGraw-Hill Book Company, Inc., 1969, pp. 336-339.
12. V. H. Ransom, et al., RELAP5/MOD1 Code Manual Volume 1: System Models and Numerical Methods, NUREG/CR-1826, EGG-2070, March 1982.

APPENDIX A

SEMISCALE MOD-2A SYSTEM AND EXPERIMENTAL DESCRIPTION

The Semiscale Mod-2A¹ system (Figure A-1) is a two-loop large pressurized water reactor (PWR) primary coolant system simulator located at the Idaho National Engineering Laboratory (INEL). One loop (intact loop) is scaled to simulate three loops of a LPWR, while the other (broken loop) simulates a single loop in which a postulated break is simulated. The system primary coolant volume and core power are scaled by approximately 1/1700. Geometric similarity and component layout have been maintained between the Mod-2A system and a LPWR. Specific similarities include a full-elevation (3.66 m), electrically heated core, full-length upper plenum and upper head, two full-elevation steam generators, and the preservation of the relative elevations of various components. ECC systems include a high pressure injection system (HPIS), passive accumulators, and a low pressure injection system (LPIS), each of which inject coolant (approximately 300 K) into the cold leg of the intact and broken loop.

The electrically heated core consists of 25 rods in a 5 x 5 matrix (1.43 cm pitch). Two rods in opposite corners are unpowered and the remaining 23 rods are powered equally yielding a flat radial profile. The axial power profile is a 12-step chopped cosine.

Each steam generator is scaled with respect to both primary and secondary coolant volumes. The intact loop generator contains six U-tubes and the broken loop contains two U-tubes. The secondary side of both generators consists of a rising (boiler) section, steam separator and downcomer. Feedwater enters the downcomer and steam exits the top of the steam generator.

The reactor vessel simulator is multi-sectional consisting of an upper head, upper plenum, heated core region, lower plenum, and an external inlet annulus and downcomer pipe. The complete pressure vessel, shown in Figure A-2, is approximately 10 m in length. The upper head accounts for about the top 25% of the pressure vessel length and volume. Included in

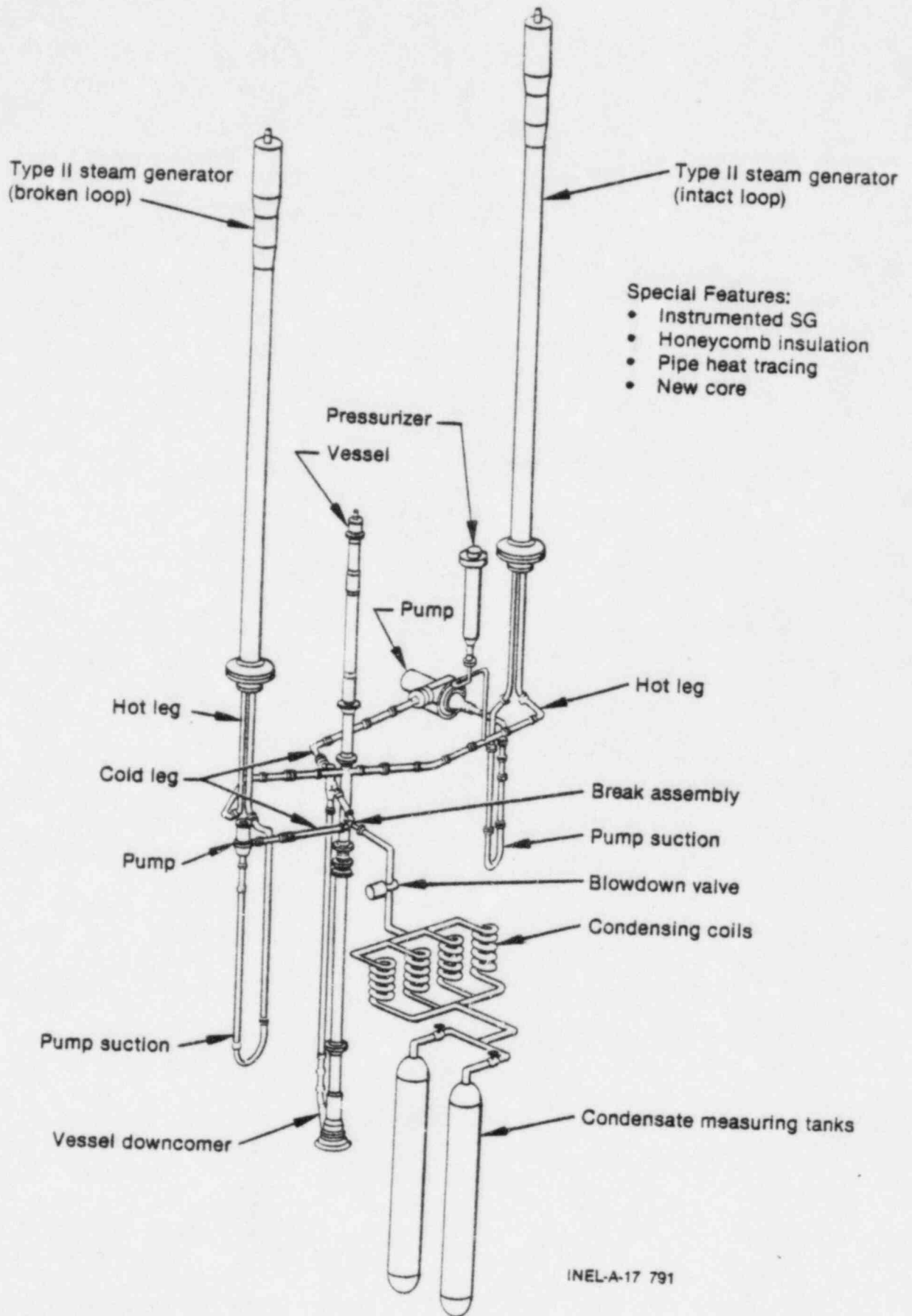


Figure A-1. Semiscale Mod-2A Facility (cold leg break configuration).

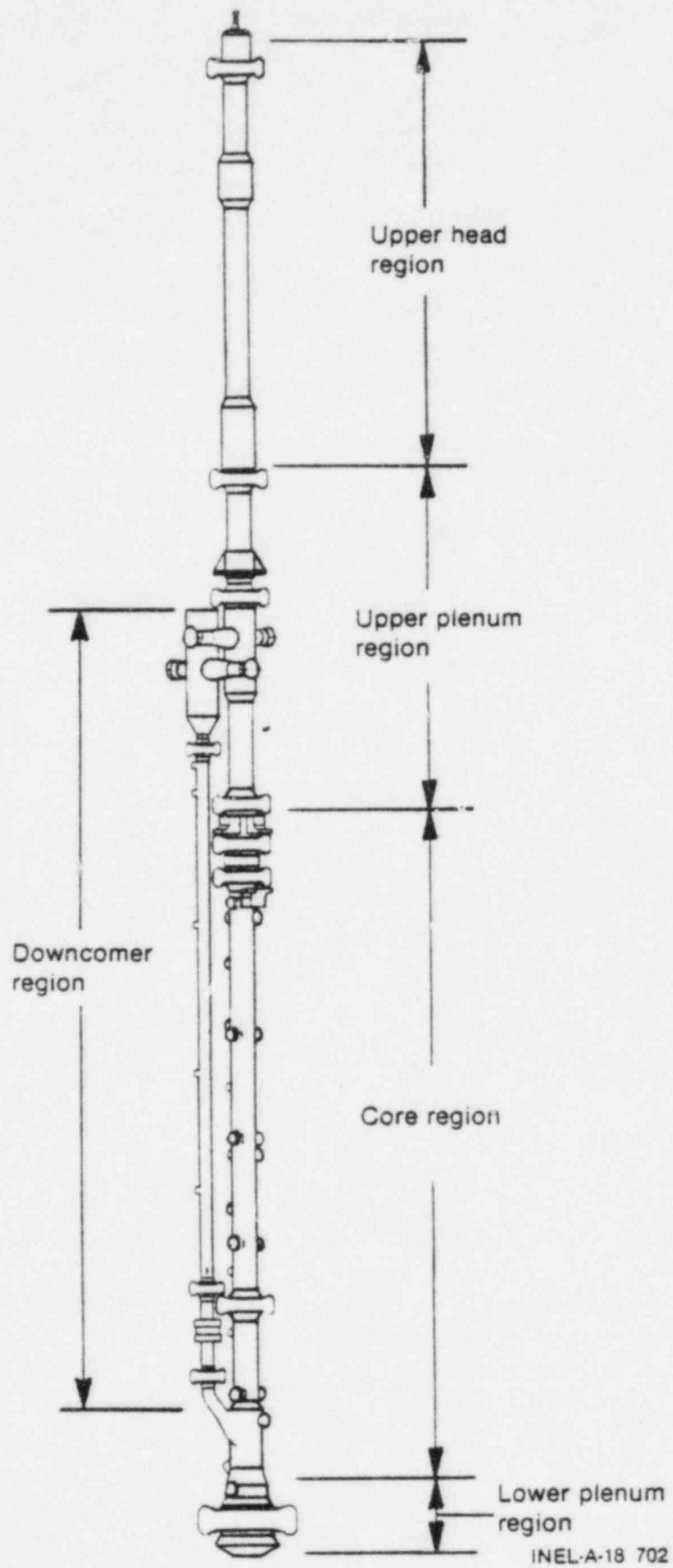


Figure A-2. Semiscale Mod-2A System reactor vessel assembly.

the upper head, are the following: a filler piece to provide proper upper head liquid volume, a simulated control rod guide tube, and two simulated support columns. The upper core support plate (simulator) forms the boundary between the upper head and upper plenum. The guide tube and the two core support columns penetrate through the upper core support plate extending into the upper plenum region.

A small line, connecting the vessel downcomer inlet annulus to the upper head simulates the bypass flow paths within a LPWR vessel. A remote control valve is installed in the bypass line for adjustment of the bypass flow and bypass line hydraulic resistance. The bypass standpipe (within the upper head) was shortened in Test S-UT-8, relative to Test S-UT-6, to obtain a fluid volume above the top of the standpipe equivalent to the scaled inverted top hat volume above the PWR downcomer bypass nozzles. Eight 7.67 mm diameter holes were drilled in a 6.3 cm section of the guide tube below the upper support plate for Test S-UT-8 which were not present in Test S-UT-6. An orifice in the guide tube was enlarged in Test S-UT-8 to 9.98 mm diameter (from 9.12 mm in Test S-UT-6) to reduce the guide tube hydraulic resistance to 9.3% of the bypass line resistance. The support columns were plugged in Test S-UT-8, so that all flow between the upper head and upper plenum must pass through the guide tube. The support columns were open to fluid flow in Test S-UT-6.

REFERENCE

- A-1. System Design Description for the Mod-2A Semiscale System, Addendum I,
"Mod-2A Phase I Addendum to Mod-3 System Design Description,
EG&G Idaho, Inc., December 1980.

APPENDIX B

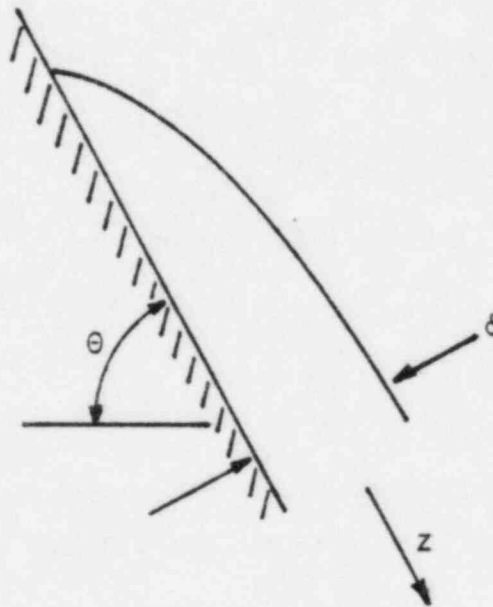
CONDENSATION

Nusselt Analysis for Laminar Condensation in the Intact Loop Steam Generator U-tubes:

The derivation of the average wall heat transfer coefficient (\bar{h}) for laminar condensation on an inclined surface results in (Collier¹):

$$1. \quad \bar{h} = 0.943 \left[\frac{\rho_f (\rho_f - \rho_g) g \sin \theta h_{fg} k_f^3}{\mu z \Delta T} \right]^{1/4}$$

where the geometry is defined by:



The film Reynolds number (Re_{film}) is determined by:

$$2. \quad Re_{film} = \frac{4\Gamma z}{\mu_f} = \frac{4}{\mu_f} \int_0^z \frac{k_f}{\delta h_{fg}} \Delta T dz$$

where the film thickness (δ) is defined by:

$$3. \quad \delta = \left[\frac{4 \mu_f k_f z \Delta T}{g \sin \theta h_{fg} \rho_f (\rho_f - \rho_g)} \right]^{1/4}$$

Combining Equations 2 and 3 and integrating:

$$4. \quad Re_{film} = \frac{4 \bar{h} z \Delta T}{\mu_f h_{fg}}$$

For this analysis, consider fluid properties at 6.9 MPa:

$$\rho_f = 742 \text{ kg/m}^3$$

$$h_{fg} = 1.512 \times 10^6 \text{ J/kg}$$

$$\rho_g = 36 \text{ kg/m}^3$$

$$\mu_f = 9.159 \times 10^{-5} \text{ kg/m-s}$$

$$k_f = 0.579408 \text{ W/m-K}$$

The differential temperature (ΔT) for the derivation of Equation 1 was defined as:

$$\Delta T = T_{fluid} - T_{wall}$$

Since no wall temperature measurements were available, T_{wall} is assumed to equal T_{fluid} on the secondary coolant side. Therefore;

$$5. \quad \Delta T = T_{primary} - T_{secondary}$$

and,

$$6. \quad \bar{h} = 10.68 \left[\frac{1}{z \Delta T} \right]^{1/4} \text{ kW/m}^2\text{-K}$$

If all core power was dissipated by vapor generation, and 3/4 of the steam flows into the intact loop:

$$\dot{m}_{\text{steam}} = \frac{0.75 Q_{\text{core}}}{h_{fg}}$$

For all the steam to be condensed:

$$7. \quad 0.75 Q_{\text{core}} = Q_{\text{condense}} = \bar{h} \Delta T A_{\text{wall}}$$

$$\text{where } A_{\text{wall}} = 6 \pi D L$$

Therefore, the tube length (L) required to condense all of the steam is:

$$8. \quad L = \frac{0.75 Q_{\text{core}}}{\bar{h} \Delta T 6 \pi D}$$

Combining Equations 6. and 8.

$$9. \quad L = \left[\frac{0.75 Q_{\text{core}}}{6 (10.68) \pi D (\Delta T)^{0.75}} \right]^{1.33}$$

By rearranging Equation 9, the minimum ΔT required to condense the total steam flow in the upflow side of the U-tubes may be calculated:

$$10. \quad \Delta T_{\text{min}} = \left[\frac{0.75 Q_{\text{core}}}{6. (10.68) \pi D (L_{\text{mean}})^{0.75}} \right]^{1.33}$$

where L_{mean} is the mean U-tube height = 9.27 m. At 3.1% full core power:

$$\Delta T_{\text{min}} = 2.86 \text{ K}$$

and

$$\bar{h} = 4.7 \text{ kW/m}^2\text{-K}$$

Figure B-1 indicates a ΔT greater than 10 K was measured over the period of interest (50 to 100 s). However, if the film Reynolds number or the vapor core Reynolds number were calculated, turbulent conditions are predicted:

$$Re_{\text{film}} = 3600$$

$$Re_{\text{vapor}} = 1700$$

Therefore, a condensation model which accounts for interfacial shear will be used to better approximate the hydraulic conditions.

Carpenter and Colburn² suggested:

$$11. \quad \bar{h} = 0.065 \left[\frac{k \rho}{\mu} \right]_f^{1/2} \left[\frac{C_p \mu}{k} \right]_f^{1/2} \tau_i^{1/2}$$

where

$$\tau_i = f_i \frac{\bar{G}_g^2}{2 \rho_g}$$

$$\bar{G}_g = 0.58 G_{\text{vapor}} \text{ for total condensation}$$

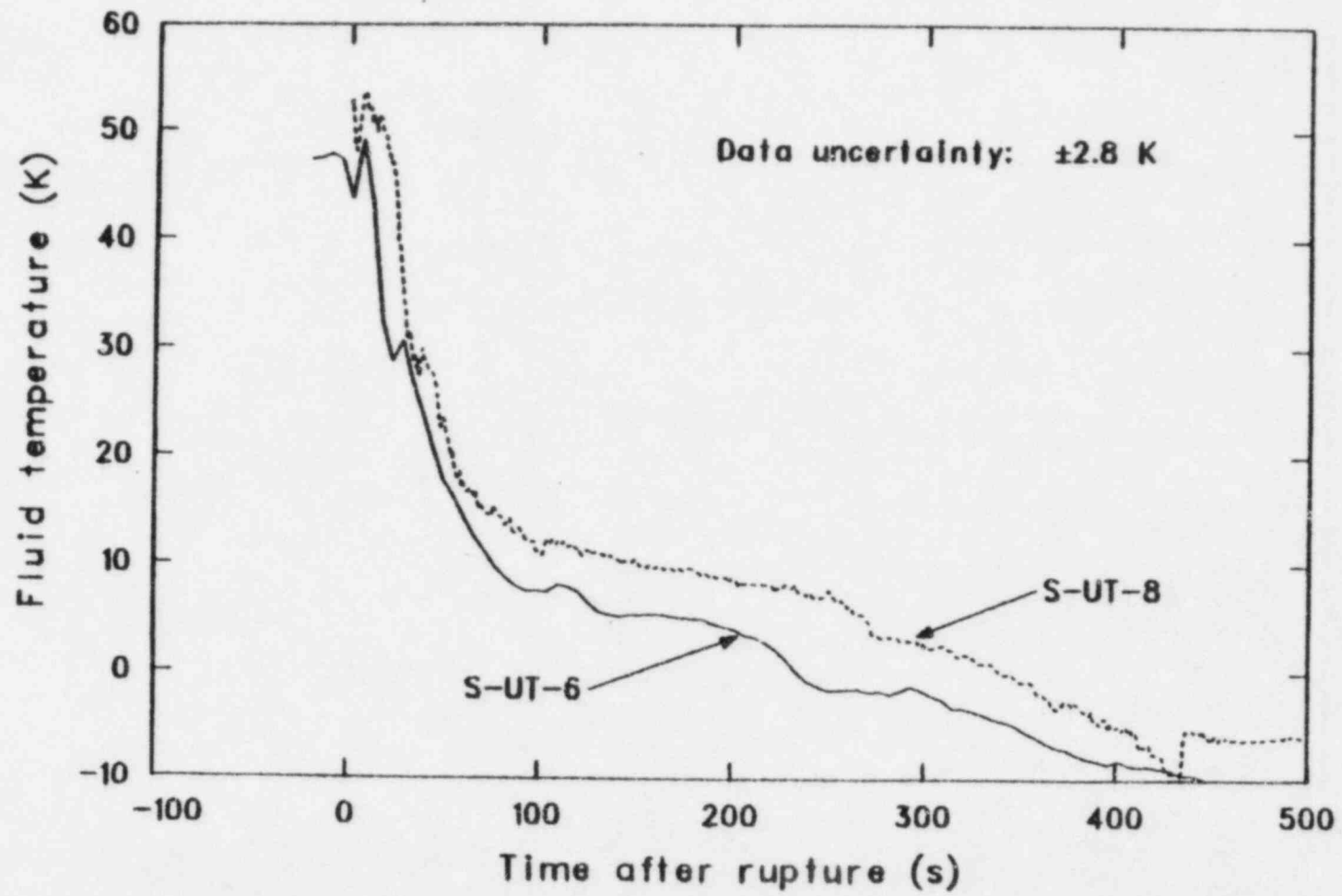


Figure B-1. Primary/secondary fluid differential temperature (30 cm above tube sheet-upflow).

Assume interfacial friction factor (f_i) may be approximated with
Balsius' Equation:

$$12. \quad f_i = 0.079 \operatorname{Re}_g^{-1/4} = 0.079 \left[\frac{\bar{G}_g D_H}{\mu_g} \right]^{-1/4}$$

Additional properties at 6.9 MPa:

$$C_p = 5204.9 \text{ J/kg-K}$$

$$\mu_g = 1.9 \times 10^{-5} \text{ kg/m-s}$$

Thus,

$$f_i = 0.0079$$

$$\bar{h} = 1.03 \text{ kW/m}^2 - \text{k}$$

This result is much lower than the Nusselt approach.

Using the Carpenter-Colburn coefficient in Equation 8, the minimum ΔT required to condense all steam in the upflow side of the U-tubes is calculated:

$$\Delta T_{\min} = 13.1 \text{ K}$$

REFERENCES

- B1. J. G. Collier, Convective Boiling and Condensation, London: McGraw-Hill Book Company (UK) Limited, 1972.
- B2. E. F. Carpenter, A. P. Colburn, "The Effect of Vapor Velocity on Condensation Inside Tubes," Proc. of General Discussion on Heat Transfer, Inst. Mechanical Engineers/ASME, pp. 20-26, 1951.

APPENDIX C

U-TUBE FLOODING IN SEMISCALE EXPERIMENTS S-UT-6 AND S-UT-8

Assuming that all core power is dissipated by vapor generation (latent heat), and three-fourths of the vapor mass flux flows into the intact loop, a maximum U-tube vapor velocity may be calculated. An additional assumption of importance for this analysis is that if n% of the total loop flow was bypass flow at steady state, then n% of the core-produced vapor flow is vented through the bypass path (therefore, not contributing to the U-tube vapor velocity). An equation for the intact loop U-tube average vapor velocity may then be written as,

$$1. \quad j_g = (1 - N) (0.75) \frac{Q_{\text{core}}}{h_{fg} \rho_v A_{\text{U-tubes}}}, \text{ where } N = \frac{n}{100}$$

$$Q_{\text{core}} = \text{Core power}$$

$$h_{fg} = \text{Latent heat of vaporization}$$

$$\rho_v = \text{Vapor density}$$

$$A_{\text{U-tube}} = \text{Total U-tube flow area}$$

The flooding velocity (j_g^{crit}) for the thermodynamic conditions and U-tube geometry can be estimated using the Wallis¹ correlation:

$$2. \quad j_g^{\star 1/2} + m |j_f^{\star}|^{1/2} = C$$

where $m = 1.0$ for turbulent flow and C is chosen as 0.725 to account for the sharp-edged U-tube entrance, and,

$$j_i^* = \frac{j_i (\rho_i)^{1/2}}{[g D (\rho_f - \rho_g)]^{1/2}}$$

Defining "flooded" as that condition in which the rising vapor mass flux is at least as large as the descending liquid mass flux

$[j_g \rho_g \geq -j_f \rho_f]$ yields an expression for the critical vapor superficial velocity:

$$j_g^{\text{crit}} = [g D (\rho_f - \rho_g)]^{1/2} \left[\frac{C}{(\rho_g)^{1/4} + (\rho_f)^{1/4} \frac{\rho_g}{\rho_f}} \right]^2$$

Equations 1 and 3 were used to yield a comparison of the estimated superficial vapor velocity and corresponding flooding velocity in each experiment. These comparisons are shown in Figures C-1 and C-2 for Tests S-UT-6 and S-UT-8, respectively.

The potential for flooding in the U-tubes is calculated through approximately 90 s after rupture in Test S-UT-6 and 110 s after rupture in S-UT-8. The significance of this result is that a flooded condition is calculated for approximately 20 s longer in Test S-UT-8 than in S-UT-6, and the only significant change in the two comparisons is the amount of vapor assumed to be vented through the bypass line.

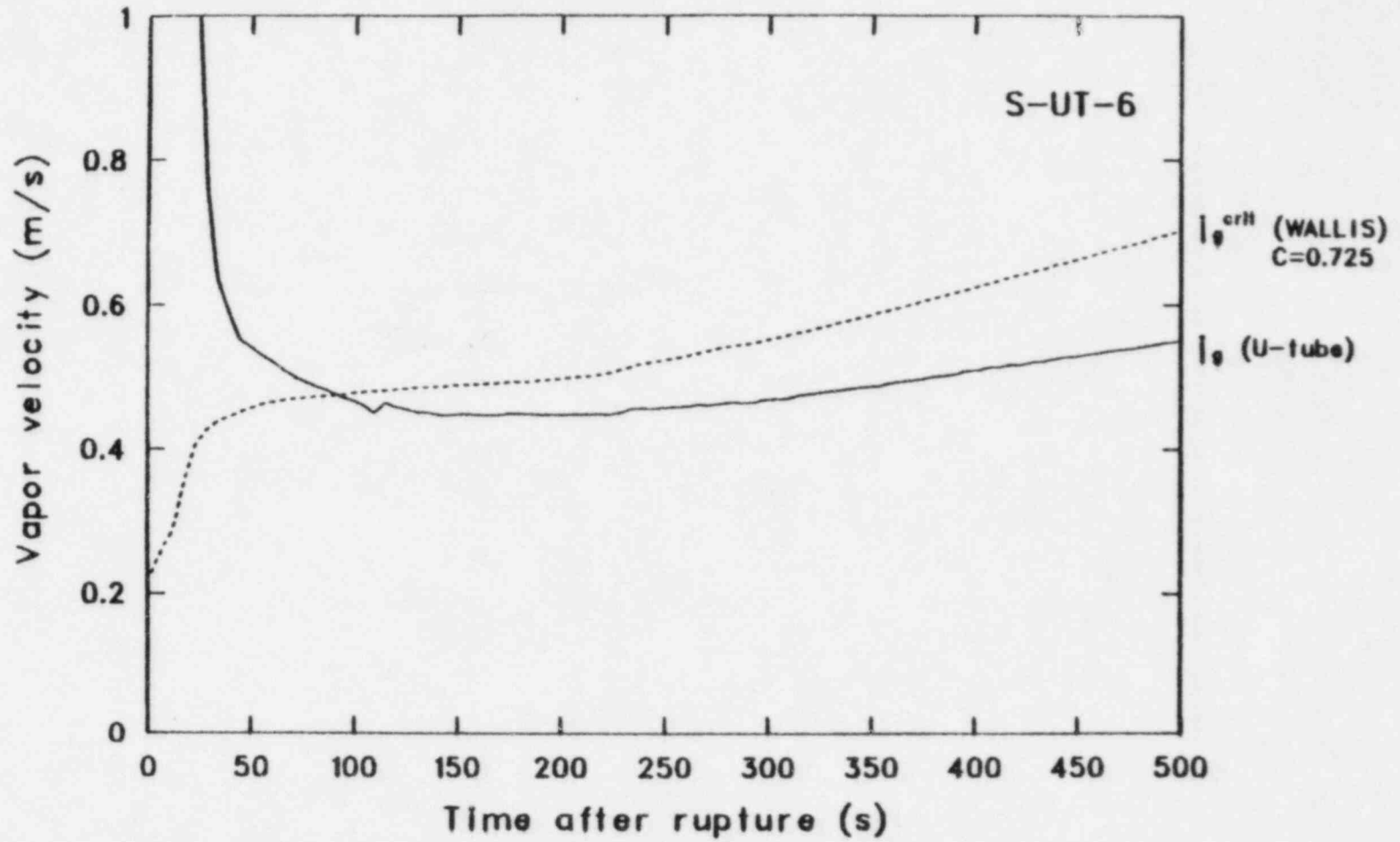


Figure C-1. Calculated intact loop U-tube vapor velocity and flooding velocities (S-UT-6).

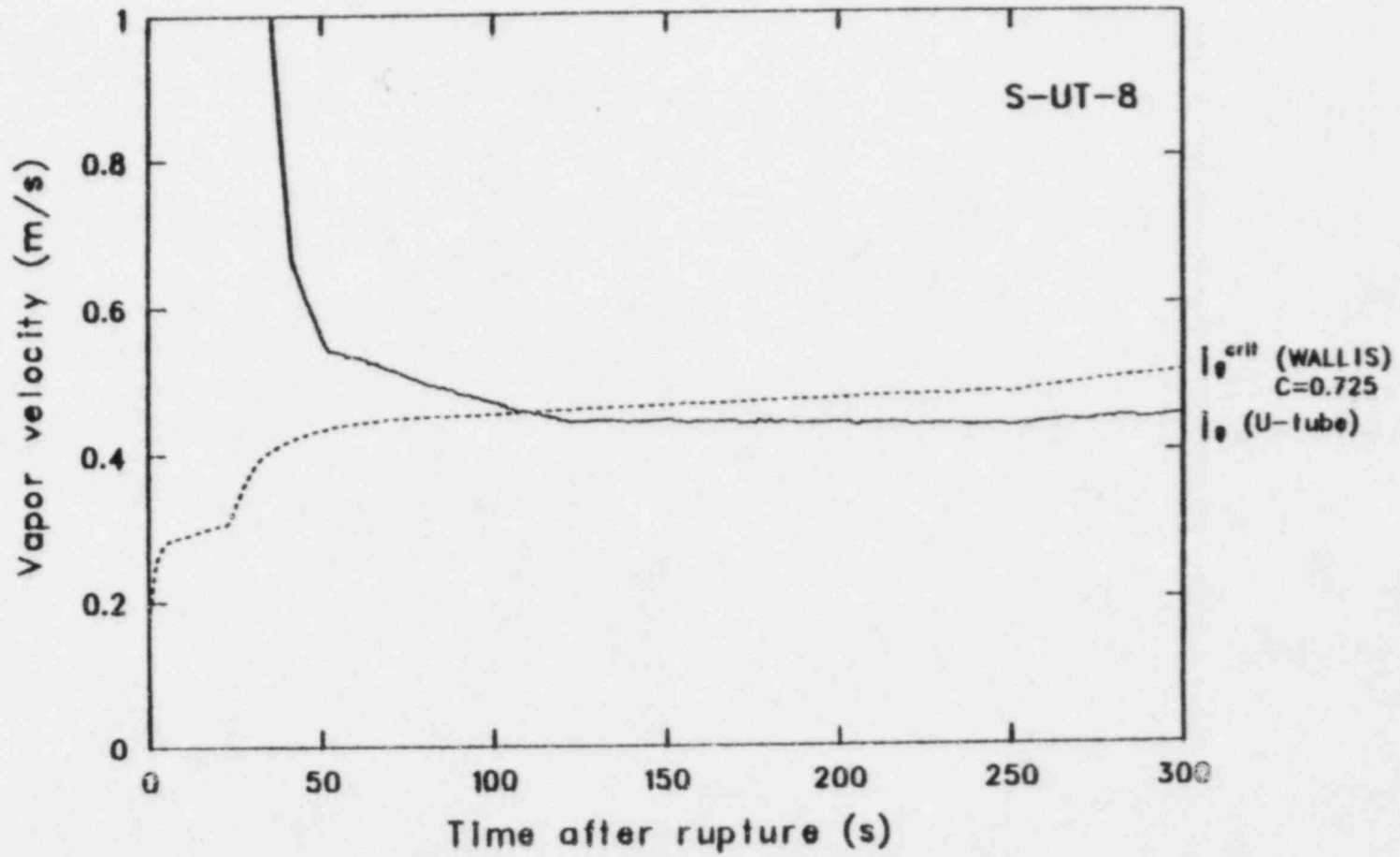


Figure C-2. Calculated intact loop U-tube vapor velocity and flooding velocities (S-UT-8).

REFERENCE

C-1. G. B. Wallis, One-Dimensional Two-Phase Flow, New York: McGraw-Hill
Book Company, Inc., 1969.